NAVAL POSTGRADUATE SCHOOL

MONTEREY, CALIFORNIA

THESIS

CONTINUED MODERNIZATION OF THE NPS TRANSONIC COMPRESSOR TEST RIG

by

Keenan S. Harman

September 2019

Thesis Advisor: Anthony J. Gannon
Second Reader: Garth V. Hobson

Approved for public release. Distribution is unlimited.

THIS PAGE INTENTIONALLY LEFT BLANK

REPORT DOCUMENTATION PAGE				*Form Approved OMB No. 0704-0188*

Public reporting burden for this collection of information is estimated to average 1 hour per response, including the time for reviewing instruction, searching existing data sources, gathering and maintaining the data needed, and completing and reviewing the collection of information. Send comments regarding this burden estimate or any other aspect of this collection of information, including suggestions for reducing this burden, to Washington headquarters Services, Directorate for Information Operations and Reports, 1215 Jefferson Davis Highway, Suite 1204, Arlington, VA 22202-4302, and to the Office of Management and Budget, Paperwork Reduction Project (0704-0188) Washington, DC 20503.

1. AGENCY USE ONLY ***(Leave blank)***	**2. REPORT DATE** September 2019	**3. REPORT TYPE AND DATES COVERED** Master's thesis

4. TITLE AND SUBTITLE CONTINUED MODERNIZATION OF THE NPS TRANSONIC COMPRESSOR TEST RIG	**5. FUNDING NUMBERS**
6. AUTHOR(S) Keenan S. Harman	
7. PERFORMING ORGANIZATION NAME(S) AND ADDRESS(ES) Naval Postgraduate School Monterey, CA 93943-5000	**8. PERFORMING ORGANIZATION REPORT NUMBER**
9. SPONSORING / MONITORING AGENCY NAME(S) AND ADDRESS(ES) N/A	**10. SPONSORING / MONITORING AGENCY REPORT NUMBER**

11. SUPPLEMENTARY NOTES The views expressed in this thesis are those of the author and do not reflect the official policy or position of the Department of Defense or the U.S. Government.

12a. DISTRIBUTION / AVAILABILITY STATEMENT Approved for public release. Distribution is unlimited.	**12b. DISTRIBUTION CODE** A

13. ABSTRACT (maximum 200 words)

The research objective of this thesis is to continue the modernization efforts of the Naval Postgraduate School's transonic compressor test rig. The current transonic compressor rig, used for testing, research and development, was built in the 1960s and operates using a compressed air turbine drive. A new design that is more efficient, more robust and less maintenance-intensive will utilize an electric drive train as the prime mover. The project is building a new rig based on the designs of the current one. This research continued to model new components using Solidworks and conducted structural and fluid flow analysis of rotating parts using ANSYS Workbench and will be used to move toward further development, manufacturing and testing of the new rig.

14. SUBJECT TERMS transonic compressor test rig, transonic compressor, compressor test rig	**15. NUMBER OF PAGES** 81
	16. PRICE CODE

17. SECURITY CLASSIFICATION OF REPORT	**18. SECURITY CLASSIFICATION OF THIS PAGE**	**19. SECURITY CLASSIFICATION OF ABSTRACT**	**20. LIMITATION OF ABSTRACT**
Unclassified	Unclassified	Unclassified	UU

NSN 7540-01-280-5500

Standard Form 298 (Rev. 2-89)
Prescribed by ANSI Std. 239-18

THIS PAGE INTENTIONALLY LEFT BLANK

CONTINUED MODERNIZATION OF THE NPS TRANSONIC COMPRESSOR TEST RIG

Keenan S. Harman
Lieutenant Commander, United States Navy
BSME, University of Wisconsin, 2007

Submitted in partial fulfillment of the
requirements for the degree of

MASTER OF SCIENCE IN MECHANICAL ENGINEERING

from the

NAVAL POSTGRADUATE SCHOOL
September 2019

Approved by: Anthony J. Gannon
Advisor

Garth V. Hobson
Second Reader

Garth V. Hobson
Chair, Department of Mechanical and Aerospace Engineering

THIS PAGE INTENTIONALLY LEFT BLANK

ABSTRACT

The research objective of this thesis is to continue the modernization efforts of the Naval Postgraduate School's transonic compressor test rig. The current transonic compressor rig, used for testing, research and development, was built in the 1960s and operates using a compressed air turbine drive. A new design that is more efficient, more robust and less maintenance-intensive will utilize an electric drive train as the prime mover. The project is building a new rig based on the designs of the current one. This research continued to model new components using Solidworks and conducted structural and fluid flow analysis of rotating parts using ANSYS Workbench and will be used to move toward further development, manufacturing and testing of the new rig.

THIS PAGE INTENTIONALLY LEFT BLANK

TABLE OF CONTENTS

THIS PAGE INTENTIONALLY LEFT BLANK

LIST OF FIGURES

LIST OF TABLES

THIS PAGE INTENTIONALLY LEFT BLANK

LIST OF ACRONYMS AND ABBREVIATIONS

Hz	Hertz
in	inches
kN	kilonewton
kW	kilowatt
m	meters
m/s	meters per second
NPS	Naval Postgraduate School
rpm	revolutions per minute
TCR	Transonic Compressor Test Rig
TPL	Turbopropulsion Laboratory

THIS PAGE INTENTIONALLY LEFT BLANK

I. INTRODUCTION

The current Naval Postgraduate School (NPS) transonic compressor test rig (TCR) has been allowing students and faculty to test, research, and develop compressor blades and stages for over five decades. Since 1968, the TCR has been a test platform for innovative flow measurements and has provided experience for graduate students to operate and test high speed compressors [1]. The legacy test rig is shown in Figure 1. Most advances in high-speed compressor fan technology have been improvements in computer simulation, however, there is still a need to test these simulations in a real-world environment and evaluate their accuracy against experimental data [2]. The NPS Turbopropulsion laboratory (TPL) is one of only a handful of facilities in the world capable of these tests: "The most amazing aspect of this rig is that it was designed on the late 60's by the late Professor Mike Vavra and the rig is still state-of-the-art today" [2].

Figure 1. Legacy Transonic Compressor Test Rig.

In order to continue to be seen as an advanced testing facility, the TCR requires a modern upgrade. The University of Notre Dame Transonic Axial Compressor facility operates a single stage axial compressor test rig driven by a DC motor [3]. Likewise, the Technische Universität Darmstadt in Darmstadt, Germany operates two high-speed compressor test rigs driven by an electrical drive [4]. Government facilities with similar capabilities include the NASA Glenn Research Center [5] and the Compressor Research Facility at the Air Force Research Laboratory at Wright-Patterson Air Force Base [6]. Each of these test rigs are driven by electric motors. The TPL has the unique distinction of being in both the government and academic sectors. The driving force for the legacy TCR is two opposed-rotor turbine stages driven with compressed air from a 12-stage Allison-Chalmers axial compressor [3]. The modern design will replace this oversized and out dated prime mover with an electric motor made by Dresser-Rand shown side by side in Figure 2.

Figure 2. Legacy 1000 kW Allison-Chalmers Compressor Versus New 300 kW Synchrony Electric Motor. Source: [1].

While reliably supporting the NPS turbomachinery laboratory for many years, the TCR has drawbacks. Based on power input to the compressor and power output of the shaft, the TCR runs at around 30% energy efficiency [1]. Likewise, the TCR has a lengthy setup process and requires around 30 minutes for the system to reach stable conditions once started. It is operated manually via a system of throttles and dump valves to control the compressed air flow from the input compressors. The control unit can be seen in Figure 3. This process is cumbersome and requires at least three people to operate. Once operating and stable, the TCR functions at a single speed, approximately 27,000 rpm, and is difficult to adjust.

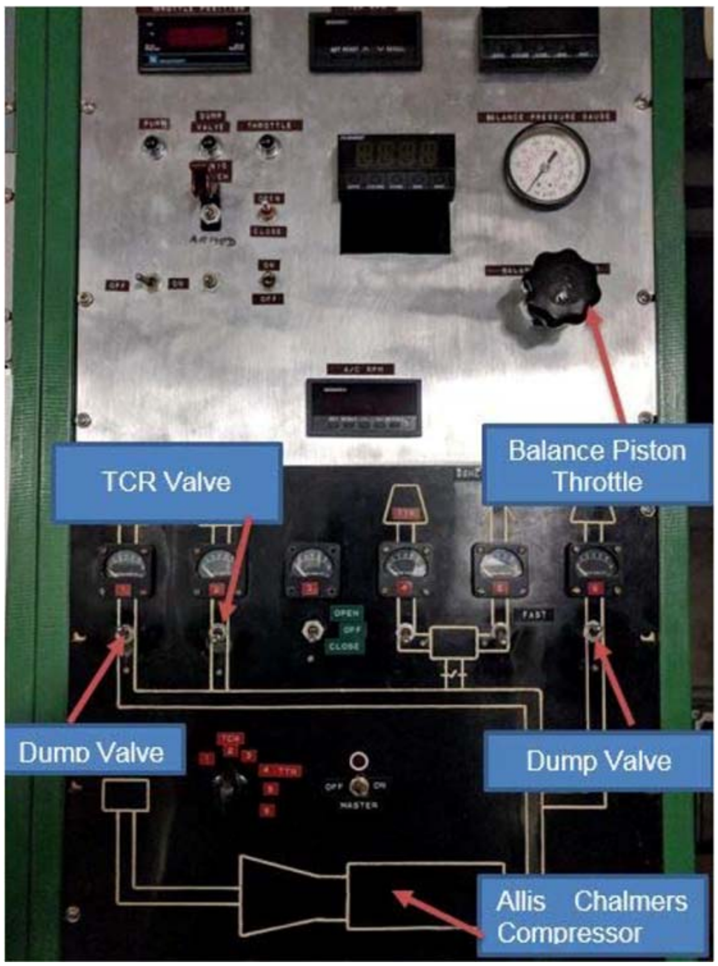

Figure 3. TCR Manual Control Unit. Source: [1].

The modernized test rig will replace the turbine drive with a 300 kW variable speed electric motor. The electric motor will be integral with the test rig and will eliminate the need for the main compressor that took up the space of an entire room next to the test cell. The new electric motor will also greatly reduce maintenance time and improve performance reliability due to the active magnetic bearing on the Synchrony motor [7]. The electric motor is expected to operate above 90 percent efficiency compared to the 30% energy efficiency of the legacy TCR [1].

Along with efficiency, the overall energy savings is large. The test rig also requires a compressor to supply air to the balance piston to remove axial thrust. Previously, a large 500 kW Elliot Compressor was used for this purpose. It has since been replaced by a 55 kW Chicago Pneumatic compressor shown side by side in Figure 4. The legacy system drew around 1500 kW between the two compressors. The new TCR will operate using around 355 kW total. It will use less energy to operate but also allows for growth in the future to test larger compressors while not needing more energy than the legacy test rig required.

Figure 4. Legacy 500 kW Elliot Compressor Versus New 55 kW Chicago Pneumatic Compressor. Source: [1].

The new motor will operate at a top speed of 21,000 rpm but can be varied to achieve desired speeds. While this is lower than the legacy test rig, the key parameter is not rotational speed of the compressor but rather tip speed of the compressor blade. In order to reach the tip speeds required to simulate operations similar to today's modern aircraft engines, the new test rig needs to be larger. Previously, compressor blades were designed to be 0.287 m (11.3 in) in diameter and the test rig could achieve a tip speed of around 405 m/s or a Mach number of 1.19. With a lower rotational speed, the new TCR was designed to be larger and more robust. A larger transmission shaft, balance piston, and support system allows compressor stages to be around 0.452 m (17.8 in) in diameter, achieving a tip speed of 495 m/s or Mach 1.45. This is a 22% higher tip speed achieved compared to the legacy test rig.

THIS PAGE INTENTIONALLY LEFT BLANK

II. DESIGN PROCESS

A. OVERVIEW

In order to maintain the TPL at NPS as a leading compressor test facility alongside the others mentioned in the introduction, the TCR modernization is vital. This research consisted of three different focus areas in order to continue the modernization of the TCR. The new rig is based off of the legacy TCR design and had already been started from previous projects, but modeling was not completed [1]. New components were designed to further the modernization. The second area was a mechanical analysis of existing modeled components using ANSYS Workbench. Specifically, the rotating transmission of the TCR was analyzed to determine deformation modes of the rig and natural frequencies that should be avoided during operation. The third focus area was a fluid analysis of flow over the balance piston to ensure adequate size of both the balance piston and the secondary compressor. A schematic of the legacy TCR facility and air supply system is shown in Figure 5 and an assembly view of the new TCR model is in Figure 6.

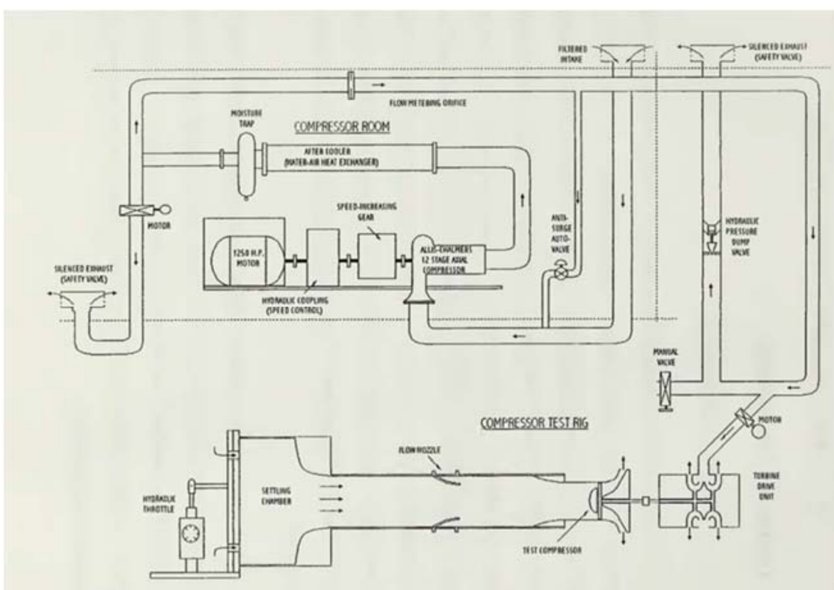

Figure 5. Legacy TCR Facility Setup. Source [1].

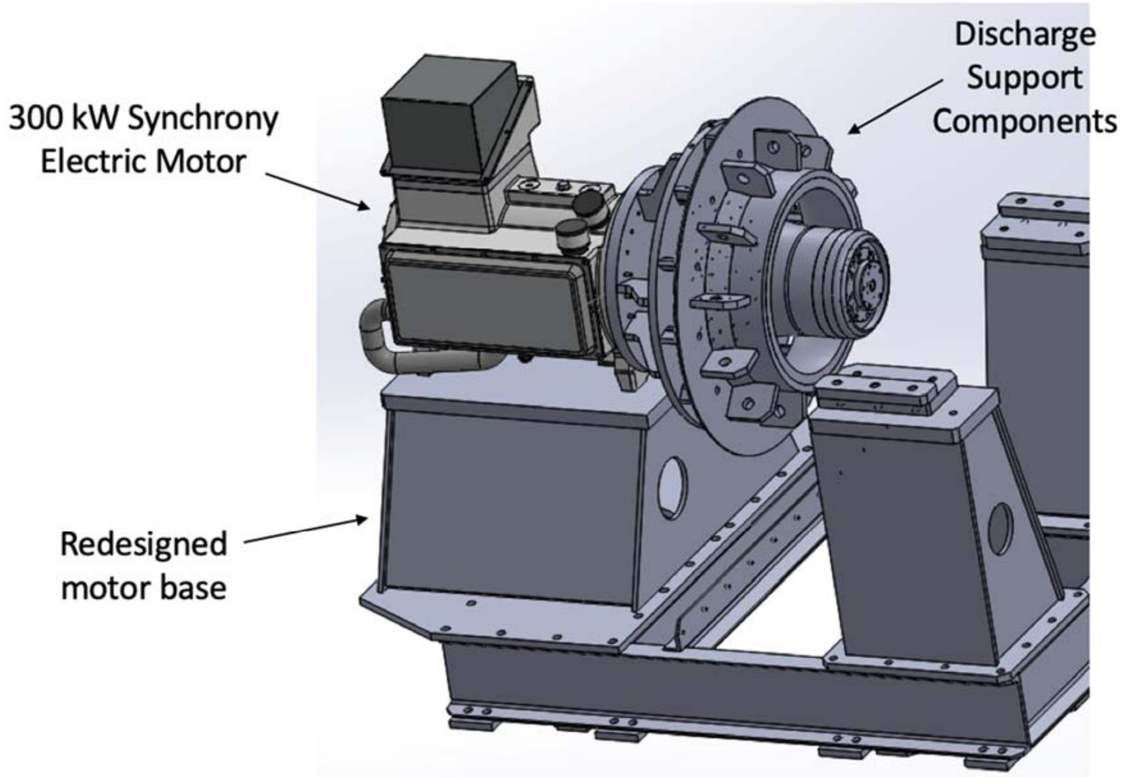

Figure 6. Assembly of Modernized TCR Model.

B. COMPONENT MODELING

Much of the new TCR had been modeled in previous work by thesis student LT Andre Byrd and Engineering Assistant Louie Duriez [1]. There was a shift in the design following LT Byrd's design for mounting of the electric motor. The back stanchions on which bear the weight of the motor were lowered from the legacy design and the motor is fix to a thick steel plate rather than resting in a cradle as in LT Byrd's design. The previous design can be seen in Figure 7. The next components to be modeled were the discharge support components of the rig. The key factors were to size the components to achieve the desired tip speed of the compressor blades and to maintain a similar flow area relationship to the legacy TCR.

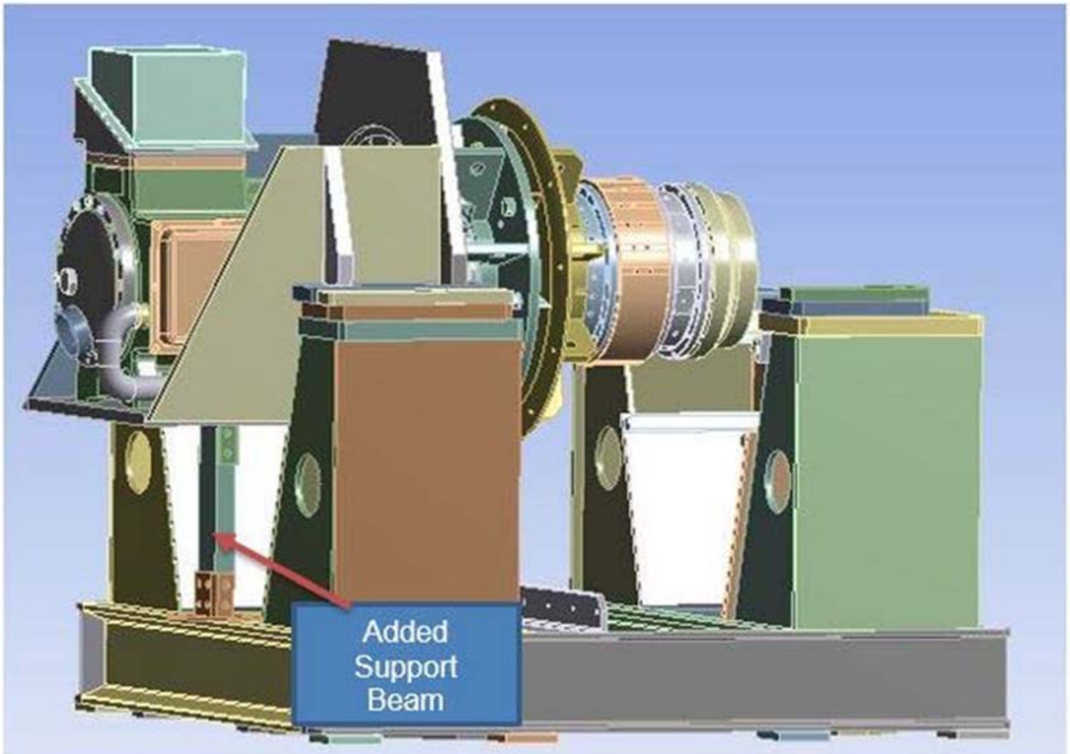

Figure 7. LT Byrd Model of Electric Motor Support and Housing.
Source: [1].

The rotational speed of the legacy TCR is 27,000 rpm, which equates to a tip speed of around 405 m/s. However, the electric motor of the modernized design has a max rotational speed of 21,000. To achieve the same tip speed as the older model, the new TCR would have to be built to a larger diameter. With the modernization, it was desired to not just meet the capabilities of the old design but to exceed them. With that in mind, the new test rig was modeled to achieve results as if the old TCR were at a speed of 33,000 rpm. The diameter of the compressor blades was increased from 0.287 m (11.3 in) to 0.452 m (17.8 in) which will allow testing of tip speeds up to 496 m/s or a Mach number of 1.45. The model of these new components can be seen in Figure 8. Once modeling was complete, the components were added to the assembly of the TCR seen in Figure 6.

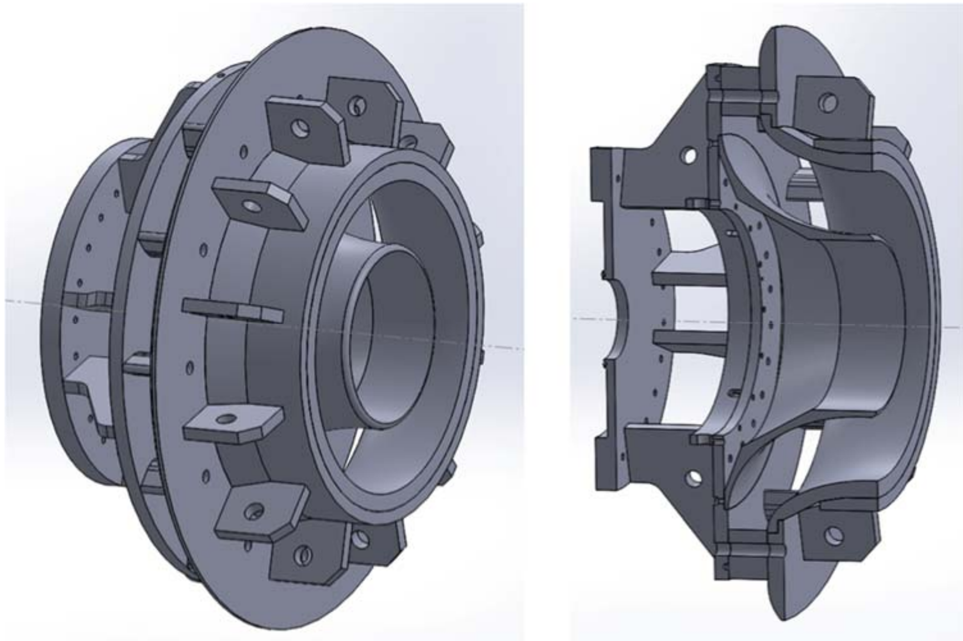

Figure 8. TCR Discharge Support Components.

C. MECHANICAL ANALYSIS

The rotating components or transmission of the new TCR were designed by Engineering Assistant Louie Duriez during his internship at NPS. A modal analysis was performed on these modeled components using ANSYS Workbench. The rotating transmission is shown in Figure 9. These are the rotating portion of the model, which can be seen highlighted in blue in Figure 10.

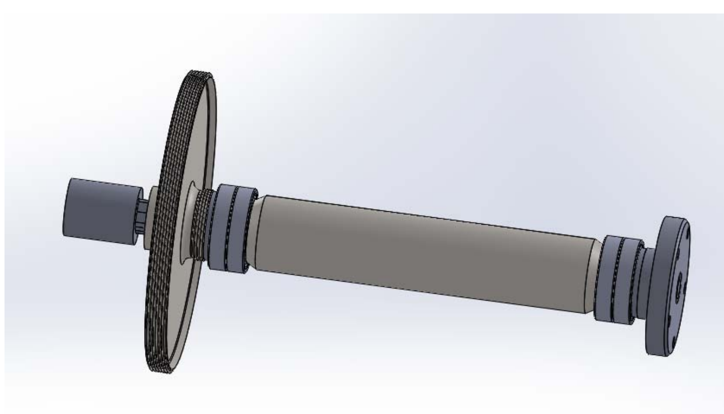

Figure 9. TCR Transmission.

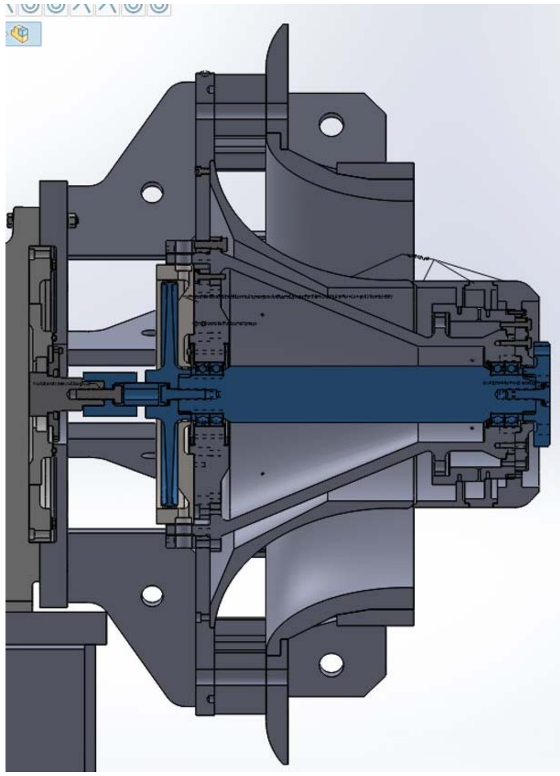

Figure 10. Cross Sectional View of the TCR with Rotating Transmission in Blue.

Analysis was started by modeling the shaft of the transmission alone to ascertain the deformation, maximum principal stress and the natural frequency modes. The test speed was set to the design rotational velocity of 21,000 rpm. A cylindrical support was placed at each end to radially support the shaft. The support closest to the balance piston also provided axial support as the balance piston prevents axial movement of the transmission. No bending constraint was applied to accurately represent bearing support boundary conditions. The shaft and the supports are shown in Figure 11.

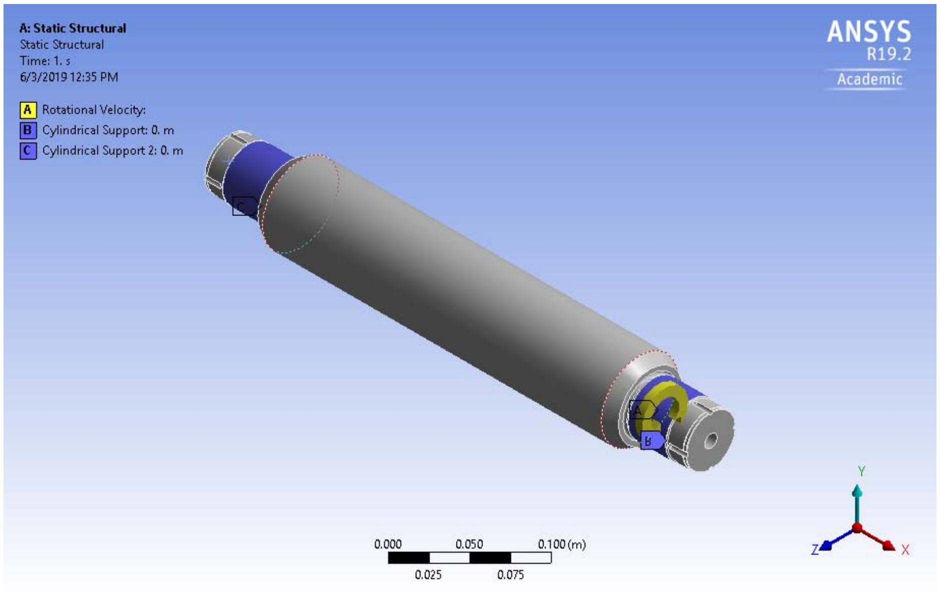

Figure 11. TCR Shaft and Supports.

The CFX solution showed bending modes for the shaft with natural frequencies around 1600 Hz. The two bending mode results are shown in Figure 12 and Figure 13. The natural frequencies of the first six modes are shown in Figure 14.

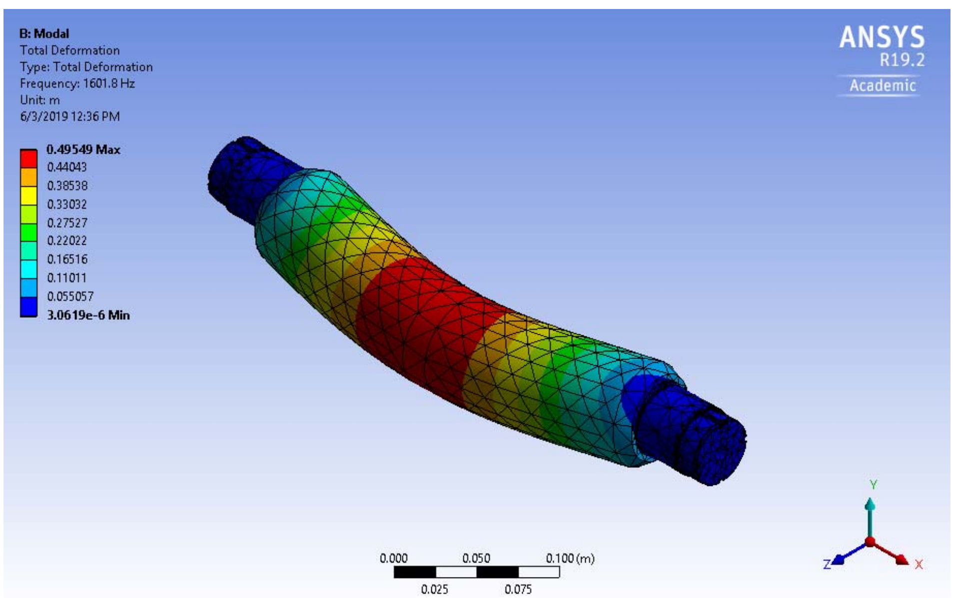

Figure 12. First Shaft Bending Mode.

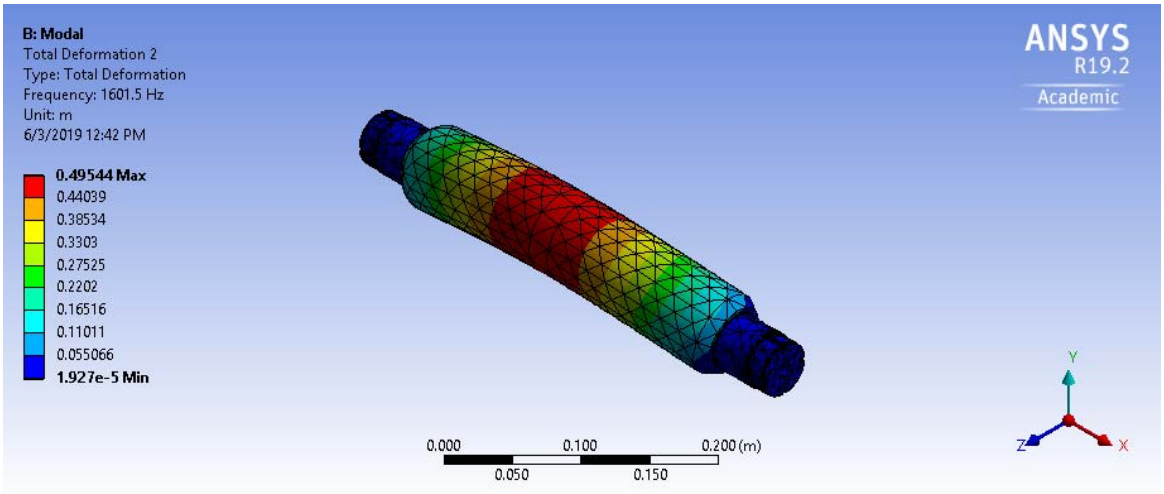

Figure 13. Second Shaft Bending Mode.

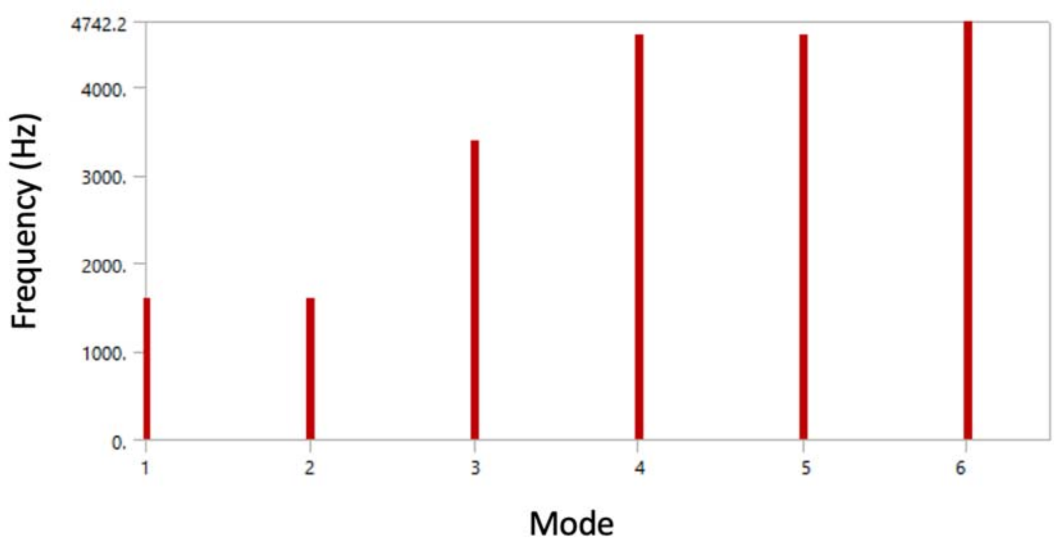

Figure 14. Natural Frequencies for Shaft.

For the next model, the rotor attachment was added to the analysis. This added mass to the components and would change the deformation modes. Again, the modes of concern were bending modes on the shaft which again occurred around a frequency of 1600 Hz, shown in Figure 15. The addition of the rotor attachment also added deformation modes not seen with the shaft alone. The first mode is believed to be a numeric anomaly and doesn't appear to represent a realistic deformation mode. Mode 2, shown in Figure 15 is the first bending mode. Examples of other modes are shown in Figure 16 and Figure 17. Figure 18 shows the natural frequencies of this configuration.

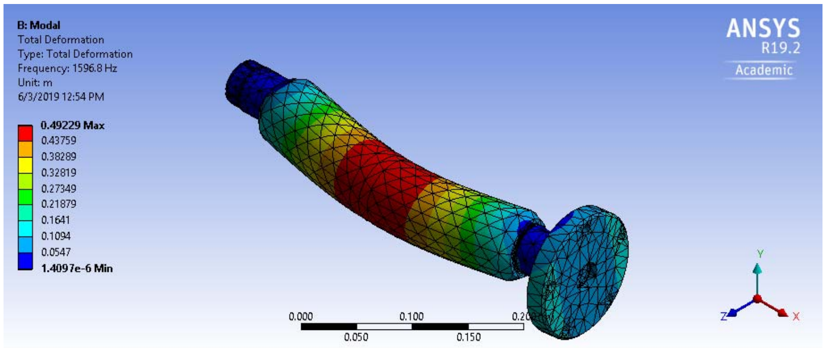

Figure 15. Bending Mode for Shaft and Rotor Attachment.

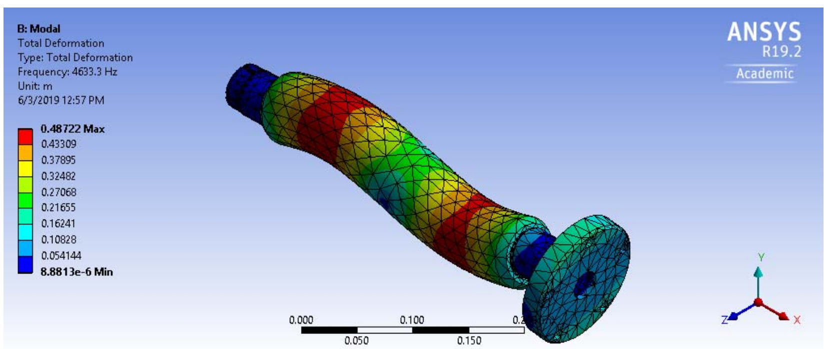

Figure 16. Additional Deformation Mode 8.

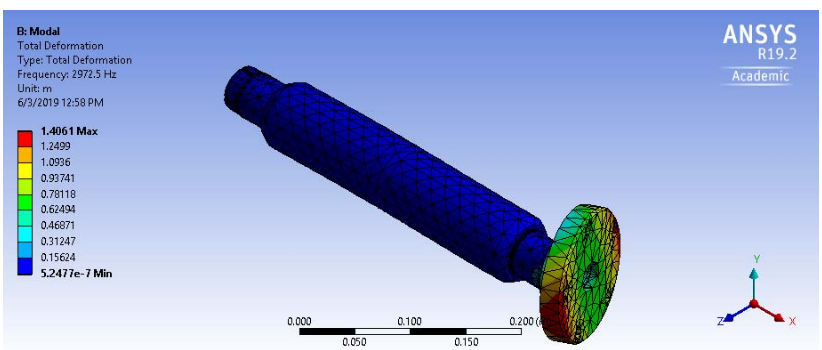

Figure 17. Additional Deformation 10.

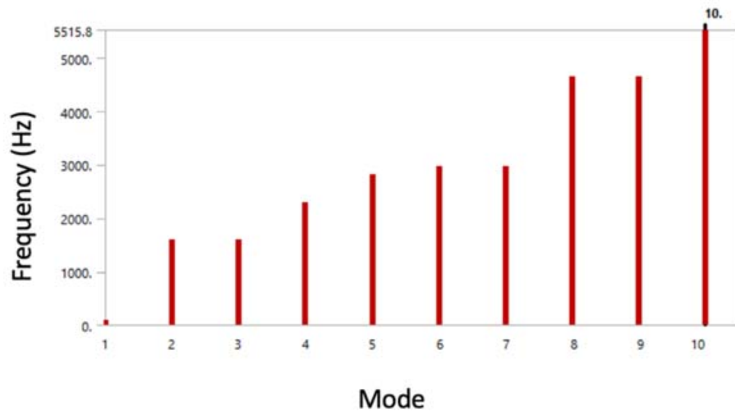

Figure 18. Natural Frequencies for Shaft and Rotor Attachment.

Lastly, the balance piston and coupling devices were added to analyze the entire transmission. The highest principal stress was found to be in the coupler and occurred at a place with a sharp angle, a typical stress concentration point, shown in Figure 19. This component could be redesigned in order to lower the stress depending on manufacturing abilities, possible with a chamfered angle instead. Similar bending modes were found on the shaft, shown in Figure 20, with a slightly raised natural frequency around 1630 Hz. Even more deformation modes were introduced centering around vibrations of the balance piston, shown in Figure 21 and Figure 22.

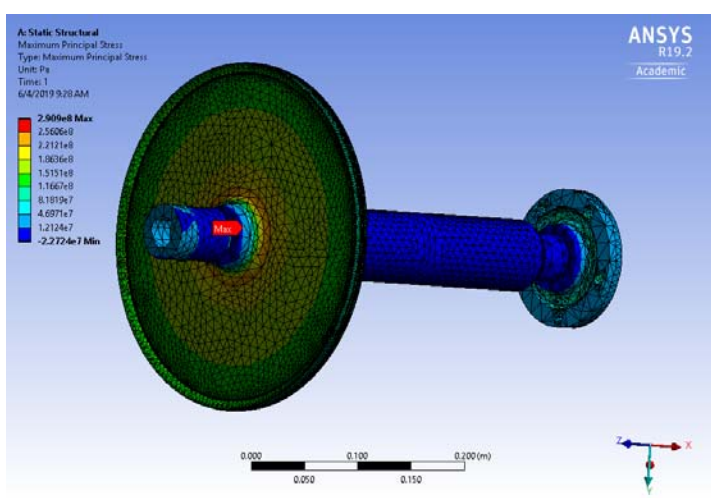

Figure 19. Maximum Principal Stress.

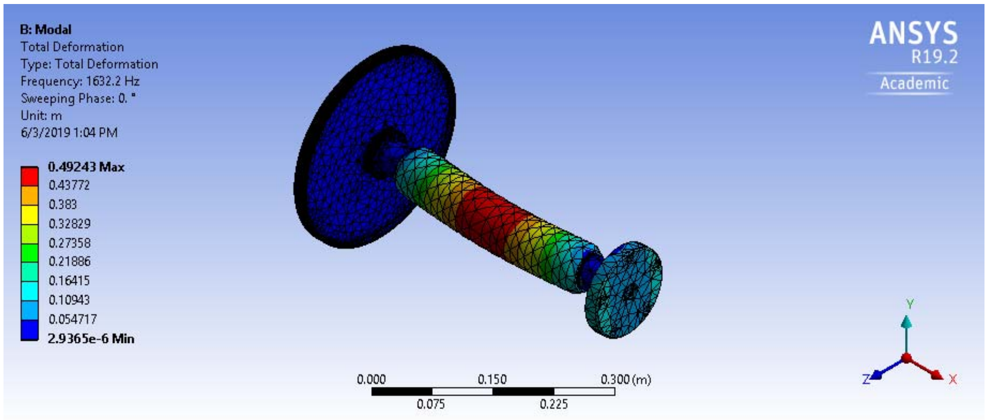

Figure 20. Bending Mode for Entire Transmission Assembly.

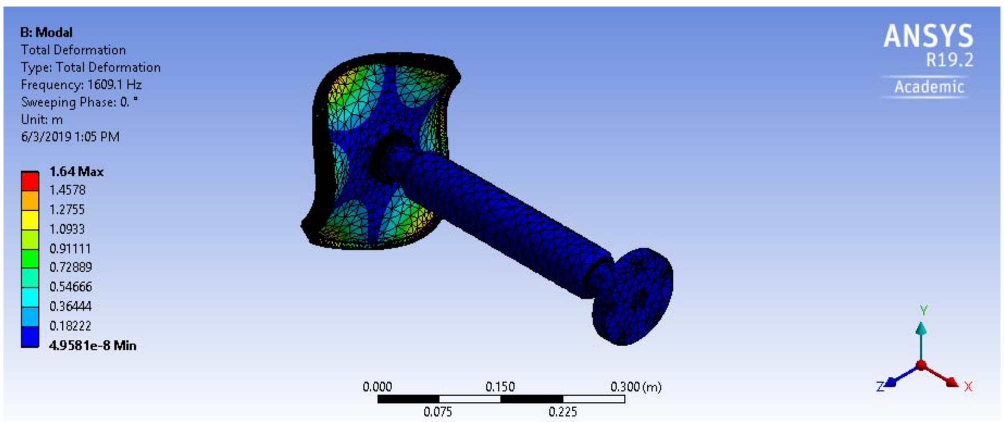

Figure 21. Additional Bending Mode 12.

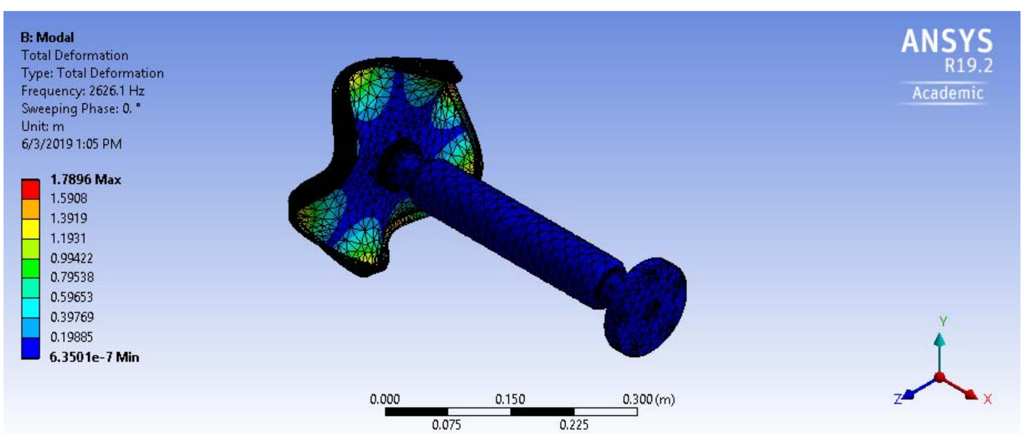

Figure 22. Additional Bending Mode 14.

A Campbell diagram for the full transmission is shown in Figure 23. This shows the natural excitation frequency versus the rotational speed of the shaft. The Campbell diagram was created in ANSYS and it shows each mode in 2000 rpm increments up to the max speed of 21,000 rpm. The black line is the engine order line. Where this line crosses the mode lines is a critical speed shown by the red triangle. This is the operating point where natural frequency of the transmission could be excited by the running speed of the rig and should be avoided. The first engine order showed no realistic critical frequencies. The second engine order is shown in the Campbell diagram in Figure 23. It crosses two different modes at the critical speed around 17,300 rpm. This speed is close to the expected operating speed of the test rig and will need closer examination to determine if it will be acceptable or if a modification to the design could change the critical speed.

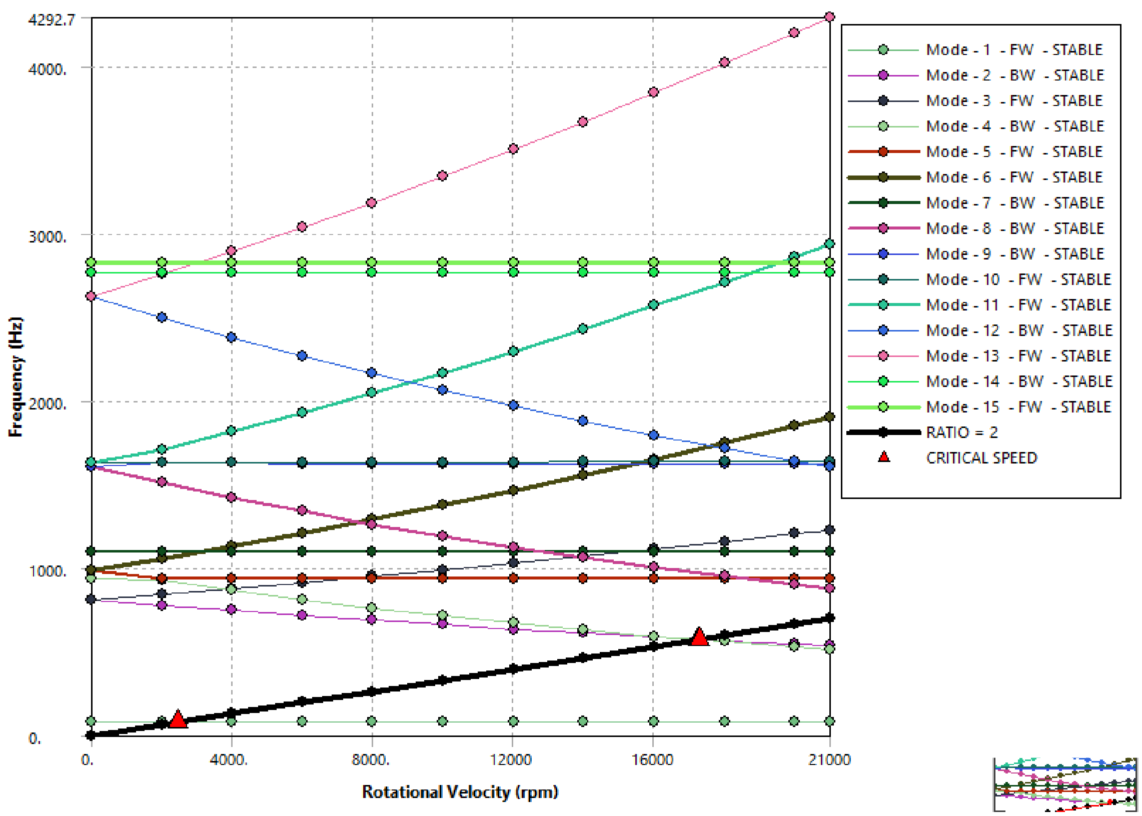

Figure 23. Campbell Diagram for Entire Transmission Analysis at 2nd Engine Order.

D. FLUID ANALYSIS

The TCR is equipped with a balance piston, shown in Figure 24, that eliminates axial thrust on the shaft and bearings caused by the test compressor when at speed. Compressed air is supplied by the secondary compressor to the right side of the balance piston and causes a force on the piston in the opposite direction from forces by the spinning test compressor blades. CFX was used to model the flow of compressed air against the balance piston and through its labyrinth seal to determine adequate size for both the compressor and balance piston.

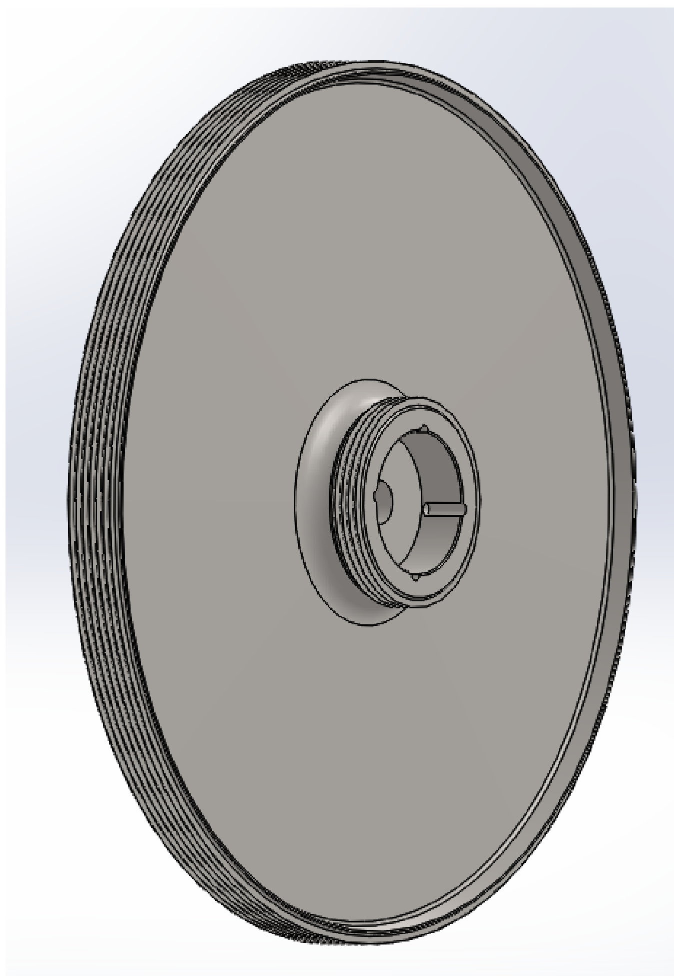

Figure 24. TCR Balance Piston.

First, the flow area around the balance piston was designed in Solidworks using the part file for the balance piston. The spacing for the labyrinth seal was set at 216 microns (0.0085 in) based on the minimum diameter tolerance for manufacture of the balance piston and maximum diameter tolerance for the casing. This would model flow through the labyrinth seal at the largest possible gap. The flow area was then reduced to a 5° slice to lower the computing time. The flow around an axis through the center of the piston is assumed to be symmetric.

In CFX, the flow inlet was set to a constant 1 bar of pressure from the compressor. The outlet was set to ambient pressure. The walls representing the casing around the balance piston were stationary while all surfaces of the rotating equipment were set to revolve at the TCR design speed of 21,000 rpm. This would simulate any flow caused by the rotating equipment. Figure 25 shows the CFX setup of the balance piston flow.

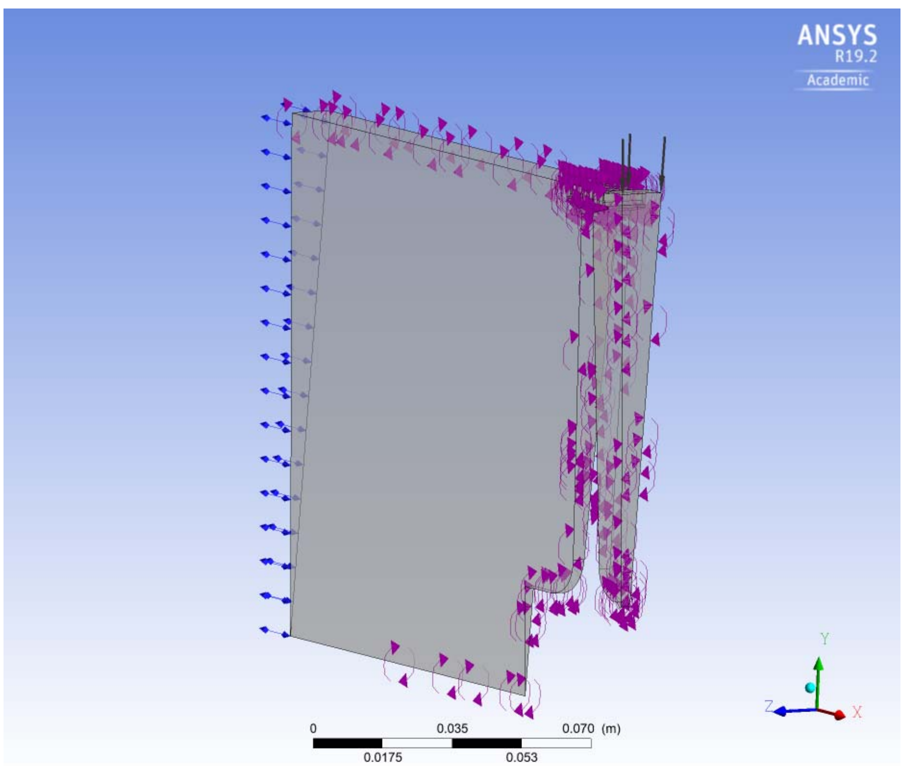

Figure 25. Flow Setup of Balance Piston Wedge.

The solution from CFX showed the flow of air into the front of the piston and the flow through the labyrinth seal. The pressure drop across the seal can be seen in Figure 26. CFX also calculated the force on the balance piston in the axial direction. Since the model was reduced to a 5° slice of the total cylinder, the force was multiplied by 72 to generate the total force on the balance piston. The air exiting the labyrinth seal remained at a subsonic velocity for the first solution set at 1 bar of pressure. Figure 27 shows the velocity gradient of the air through the seal. The flow exiting the labyrinth seal goes reaches sonic speed for all inlet pressures above 2 bar. An example is shown in Figure 28.

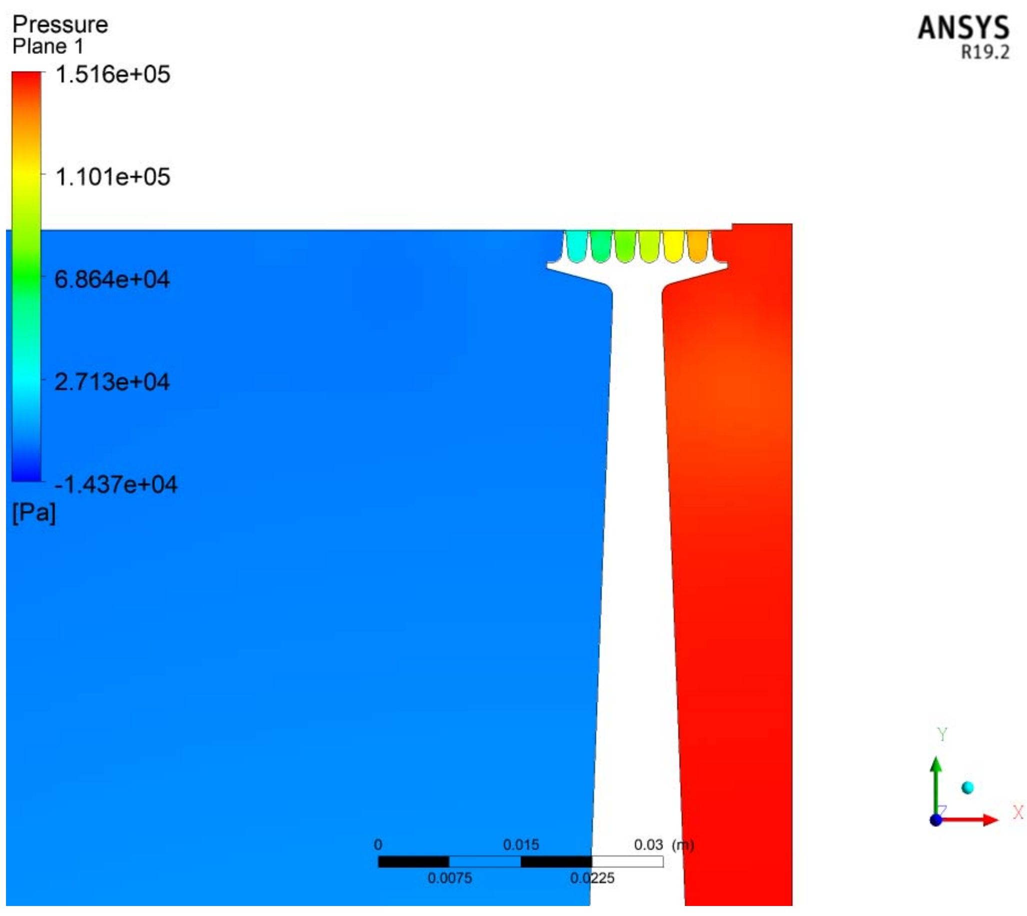

Figure 26. Pressure Drop Across Labyrinth Seal.

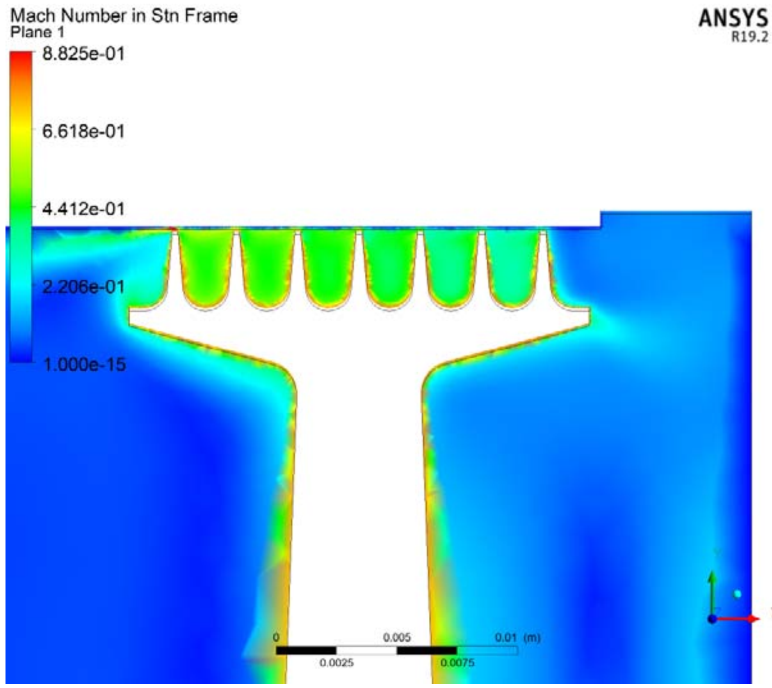

Figure 27. Mach Number Across Labyrinth Seal with Inlet Pressure of 1 Bar.

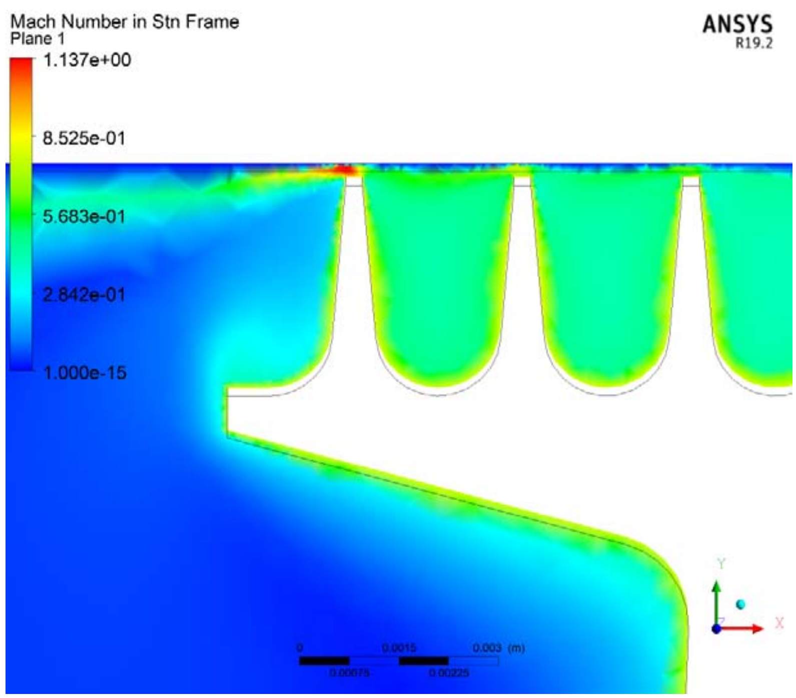

Figure 28. Supersonic Flow from Labyrinth Seal at 2 Bar Inlet Pressure

The solution was repeated in CFX using inlet pressures of 0.5, 2, 3, 5, 7.5, and 10 bar. Table 1 shows the results of total axial force on the balance piston and the Mach number of the flow exiting the labyrinth seal. The 1 bar inlet pressure setting generated a force of 7.602 kN. This value should be more than adequate to counter the axial force made by the test compressor. The air pressure from the secondary compressor has a max output of 10 bar which modeled a force on the balance piston of 64.957 kN. Since the expected thrust of from the spinning test compressor is less that 5 kN, the size of both the balance piston and the secondary air compressor are large enough to make the TCR function and allow for much larger compressor blades to be tested.

An attempt was made at this point to refine the mesh around the tip region to ensure accuracy of the calculations. The number of nodes in the mesh was increased from 266,959 to 675,950 with a negligible change to both velocity of the tip region and force on the balance piston.

Table 1. Total force and Mach Number of each Test Run

Test Pressure (bar)	0.5	1	2	3	5	7.5	10
Total Force (kN)	4.417	7.602	13.691	19.797	32.311	48.357	64.957
Mach Number	0.83	0.88	1.14	1.31	1.54	1.79	2.06

III. DISCUSSION/CONCLUSION

Once built, the modernized design of the transonic compressor test rig should be extremely beneficial to students and staff at NPS and maintain the Turbopropulsion Laboratory as a leader in high-speed compressor fan research. The new design will allow for more frequent use of a broader range of possible designs all while lowering energy consumption. The new TCR progressed towards completion with new components being modeled. Modal analysis of the rotating components of the TCR showed deformation modes of concerns and corresponding natural frequencies. This analysis will allow operators to know what frequencies are most likely to cause damage within the TCR and avoid operating at those speeds. This will ideally limit maintenance and repair costs and extend the operating life of the modernized TCR. Fluid analysis of the balance piston provided valuable data to ensure that both the secondary air compressor and balance piston are adequately sized for the new test rig.

THIS PAGE INTENTIONALLY LEFT BLANK

IV. FUTURE WORK

The Modernized TCR is very close to being fully modeled. Continued work to design the TCR should be completed so that the manufacturing stage can begin. Further mechanical analysis of the completed model of the TCR and a fluid analysis of flow through the entire rig will be necessary.

One of the issues that came up when analyzing the flow around the balance piston was the excess pressure that was created due to the rotation. This caused an anomaly where pressure in the chamber would be higher than the inlet pressure from the compressor. It warrants further investigation into whether the balance piston could be designed to use this pressure rise and eliminate the need for a compressor entirely.

THIS PAGE INTENTIONALLY LEFT BLANK

APPENDIX A. ANSYS MODAL ANALYSIS PROJECT REPORT

Project

First Saved	Wednesday, May 15, 2019
Last Saved	Wednesday, May 22, 2019
Product Version	19.2 Release
Save Project Before Solution	No
Save Project After Solution	No

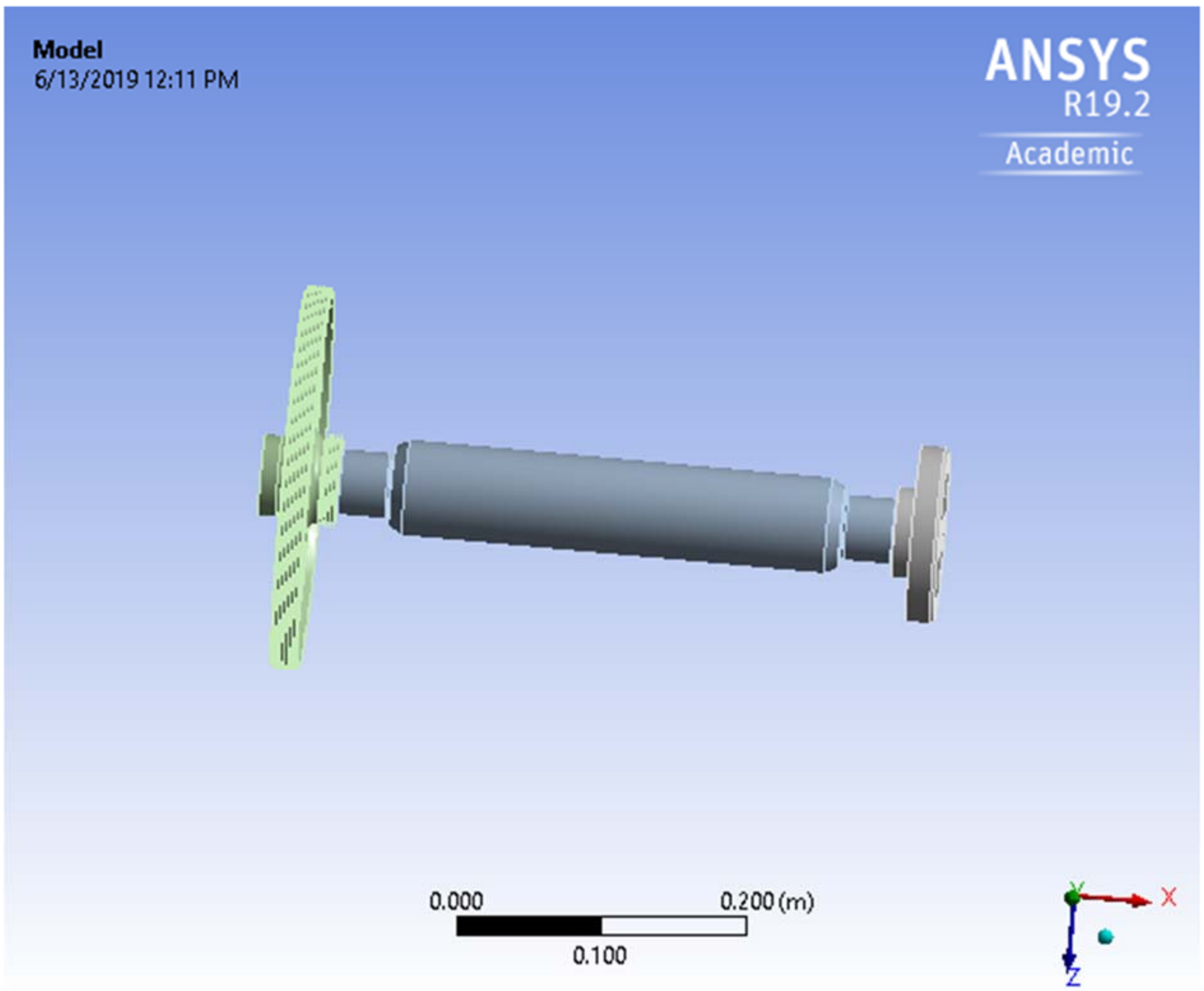

Contents

Units

TABLE 1

Unit System	Metric (m, kg, N, s, V, A) Degrees RPM Celsius
Angle	Degrees
Rotational Velocity	RPM
Temperature	Celsius

Model (A4, B4)

Geometry

TABLE 2
Model (A4, B4) > Geometry

Object Name	*Geometry*
State	Fully Defined
Definition	
Source	E:\KeenanHarman\ANSYS\shaft+rotor+balance_piston\shaft+rotor+balance_piston.x_t
Type	Parasolid
Length Unit	Meters
Element Control	Program Controlled
Display Style	Body Color
Bounding Box	
Length X	0.4714 m
Length Y	0.26645 m
Length Z	0.26645 m
Properties	
Volume	1.9559e-003 m³
Mass	15.354 kg
Scale Factor Value	1.
Statistics	
Bodies	3
Active Bodies	3
Nodes	187691
Elements	91100
Mesh Metric	None
Update Options	
Assign Default Material	No
Basic Geometry Options	
Solid Bodies	Yes
Surface Bodies	Yes
Line Bodies	No
Parameters	Independent
Parameter Key	ANS;DS
Attributes	No
Named Selections	No
Material Properties	No
Advanced Geometry Options	

Use Associativity	Yes
Coordinate Systems	No
Reader Mode Saves Updated File	No
Use Instances	Yes
Smart CAD Update	Yes
Compare Parts On Update	No
Analysis Type	3-D
Mixed Import Resolution	None
Clean Bodies On Import	No
Stitch Surfaces On Import	No
Decompose Disjoint Geometry	Yes
Enclosure and Symmetry Processing	Yes

TABLE 3
Model (A4, B4) > Geometry > Parts

Object Name	*B2103_rotor_attachment*	*B2105-1_main_drive_shafts*	*B2108-3_balance_piston*
State	Meshed		
Graphics Properties			
Visible	Yes		
Transparency	1		
Definition			
Suppressed	No		
Stiffness Behavior	Flexible		
Coordinate System	Default Coordinate System		
Reference Temperature	By Environment		
Behavior	None		

Material			
Assignment	Structural Steel		
Nonlinear Effects	Yes		
Thermal Strain Effects	Yes		
Bounding Box			
Length X	3.1979e-002 m	0.41656 m	5.334e-002 m
Length Y	0.12192 m	6.604e-002 m	0.26645 m
Length Z	0.12192 m	6.604e-002 m	0.26645 m
Properties			
Volume	2.1226e-004 m³	1.2105e-003 m³	5.3313e-004 m³
Mass	1.6663 kg	9.5023 kg	4.1851 kg
Centroid X	0.46072 m	0.24638 m	2.748e-002 m
Centroid Y	1.2463e-008 m	-2.5602e-009 m	1.1571e-007 m
Centroid Z	3.9542e-010 m	-9.5338e-011 m	-5.2754e-006 m
Moment of Inertia Ip1	2.9714e-003 kg·m²	4.6939e-003 kg·m²	2.8334e-002 kg·m²
Moment of Inertia Ip2	1.5668e-003 kg·m²	0.10696 kg·m²	1.4352e-002 kg·m²
Moment of Inertia Ip3	1.5668e-003 kg·m²	0.10696 kg·m²	1.4355e-002 kg·m²
Statistics			
Nodes	4244	11362	172085
Elements	2317	6527	82256
Mesh Metric	None		

Coordinate Systems

TABLE 4
Model (A4, B4) > Coordinate Systems > Coordinate System

Object Name	*Global Coordinate System*	*Coordinate System*
State	Fully Defined	
Definition		
Type	Cartesian	Cylindrical
Coordinate System ID	0.	
Coordinate System		Program Controlled
APDL Name		
Suppressed		No
Origin		
Origin X	0. m	
Origin Y	0. m	
Origin Z	0. m	
Define By		Global Coordinates
Location		Defined
Directional Vectors		
X Axis Data	[1. 0. 0.]	[0. -1. 0.]
Y Axis Data	[0. 1. 0.]	[0. 0. -1.]
Z Axis Data	[0. 0. 1.]	[1. 0. 0.]

Principal Axis		
Axis		Z
Define By		Global X Axis
Orientation About Principal Axis		
Axis		X
Define By		Default
Transformations		
Base Configuration		Absolute
Transformed Configuration		[0. 0. 0.]

Connections

TABLE 5
Model (A4, B4) > Connections

Object Name	*Connections*
State	Fully Defined
Auto Detection	
Generate Automatic Connection On Refresh	Yes
Transparency	
Enabled	Yes

TABLE 6
Model (A4, B4) > Connections > Contacts

Object Name	*Contacts*
State	Fully Defined
Definition	
Connection Type	Contact
Scope	
Scoping Method	Geometry Selection
Geometry	All Bodies
Auto Detection	
Tolerance Type	Slider
Tolerance Slider	0.
Tolerance Value	1.5087e-003 m
Use Range	No
Face/Face	Yes
Face Overlap Tolerance	Off
Cylindrical Faces	Include
Face/Edge	No
Edge/Edge	No
Priority	Include All
Group By	Bodies
Search Across	Bodies
Statistics	
Connections	2
Active Connections	2

TABLE 7
Model (A4, B4) > Connections > Contacts > Contact Regions

Object Name	*Contact Region*	*Contact Region 2*
State	Fully Defined	
Scope		
Scoping Method	Geometry Selection	
Contact	3 Faces	7 Faces
Target	7 Faces	
Contact Bodies	B2103_rotor_attachment	B2105-1_main_drive_shafts
Target Bodies	B2105-1_main_drive_shafts	B2108-3_balance_piston
Protected	No	
Definition		
Type	Bonded	
Scope Mode	Automatic	
Behavior	Program Controlled	
Trim Contact	Program Controlled	
Trim Tolerance	1.5087e-003 m	
Suppressed	No	
Advanced		
Formulation	Program Controlled	
Small Sliding	Program Controlled	
Detection Method	Program Controlled	
Penetration Tolerance	Program Controlled	
Elastic Slip Tolerance	Program Controlled	
Normal Stiffness	Program Controlled	
Update Stiffness	Program Controlled	
Pinball Region	Program Controlled	
Geometric Modification		
Contact Geometry Correction	None	
Target Geometry Correction	None	

Mesh

TABLE 8
Model (A4, B4) > Mesh

Object Name	*Mesh*
State	Solved
Display	
Display Style	Use Geometry Setting
Defaults	
Physics Preference	Mechanical
Element Order	Program Controlled
Element Size	Default
Sizing	
Use Adaptive Sizing	Yes
Resolution	Default (2)
Mesh Defeaturing	Yes

Defeature Size	Default
Transition	Fast
Span Angle Center	Coarse
Initial Size Seed	Assembly
Bounding Box Diagonal	0.60349 m
Average Surface Area	1.4542e-003 m²
Minimum Edge Length	5.0924e-005 m
Quality	
Check Mesh Quality	Yes, Errors
Error Limits	Standard Mechanical
Target Quality	Default (0.050000)
Smoothing	Medium
Mesh Metric	None
Inflation	
Use Automatic Inflation	None
Inflation Option	Smooth Transition
Transition Ratio	0.272
Maximum Layers	5
Growth Rate	1.2
Inflation Algorithm	Pre
View Advanced Options	No
Advanced	
Number of CPUs for Parallel Part Meshing	Program Controlled
Straight Sided Elements	No
Number of Retries	Default (4)
Rigid Body Behavior	Dimensionally Reduced
Triangle Surface Mesher	Program Controlled
Topology Checking	Yes
Pinch Tolerance	Please Define
Generate Pinch on Refresh	No
Statistics	
Nodes	187691
Elements	91100

Named Selections

TABLE 9
Model (A4, B4) > Named Selections > Named Selections

Object Name	*bearing1*	*bearing2*
State	Fully Defined	
Scope		
Scoping Method	Geometry Selection	
Geometry	1 Face	
Definition		
Send to Solver	Yes	
Protected	Program Controlled	
Visible	Yes	

Program Controlled Inflation	Exclude
Statistics	
Type	Manual
Total Selection	1 Face
Surface Area	4.5832e-003 m²
Suppressed	0
Used by Mesh Worksheet	No

Static Structural (A5)

TABLE 10
Model (A4, B4) > Analysis

Object Name	*Static Structural (A5)*
State	Solved
Definition	
Physics Type	Structural
Analysis Type	Static Structural
Solver Target	Mechanical APDL
Options	
Environment Temperature	22. °C
Generate Input Only	No

TABLE 11
Model (A4, B4) > Static Structural (A5) > Analysis Settings

Object Name	*Analysis Settings*
State	Fully Defined
Restart Analysis	
Restart Type	Program Controlled
Status	Done
Step Controls	
Number Of Steps	1.
Current Step Number	1.
Step End Time	1. s
Auto Time Stepping	Program Controlled
Solver Controls	
Solver Type	Program Controlled
Weak Springs	Off

Solver Pivot Checking	Program Controlled
Large Deflection	Off
Inertia Relief	Off
Rotordynamics Controls	
Coriolis Effect	On
Restart Controls	
Generate Restart Points	Program Controlled
Retain Files After Full Solve	Yes
Combine Restart Files	Program Controlled
Nonlinear Controls	
Newton-Raphson Option	Program Controlled
Force Convergence	Program Controlled
Moment Convergence	Program Controlled
Displacement Convergence	Program Controlled
Rotation Convergence	Program Controlled
Line Search	Program Controlled
Stabilization	Off
Output Controls	
Stress	Yes
Strain	Yes
Nodal Forces	No
Contact Miscellaneous	No

General Miscellaneous	No
Store Results At	All Time Points
Analysis Data Management	
Solver Files Directory	E:\KeenanHarman\ANSYS\shaft+rotor+balance_piston\shaft+rotor+balance_piston_files\dp0\SYS\MECH\
Future Analysis	Prestressed analysis
Scratch Solver Files Directory	
Save MAPDL db	No
Contact Summary	Program Controlled
Delete Unneeded Files	Yes
Nonlinear Solution	No
Solver Units	Active System
Solver Unit System	mks

TABLE 12
Model (A4, B4) > Static Structural (A5) > Rotations

Object Name	*Rotational Velocity*
State	Fully Defined
Scope	
Scoping Method	Geometry Selection
Geometry	All Bodies
Definition	
Define By	Components
Coordinate System	Global Coordinate System
X Component	21000 RPM (ramped)
Y Component	0. RPM (ramped)
Z Component	0. RPM (ramped)
X Coordinate	0. m
Y Coordinate	0. m
Z Coordinate	0. m
Suppressed	No

FIGURE 1
Model (A4, B4) > Static Structural (A5) > Rotational Velocity

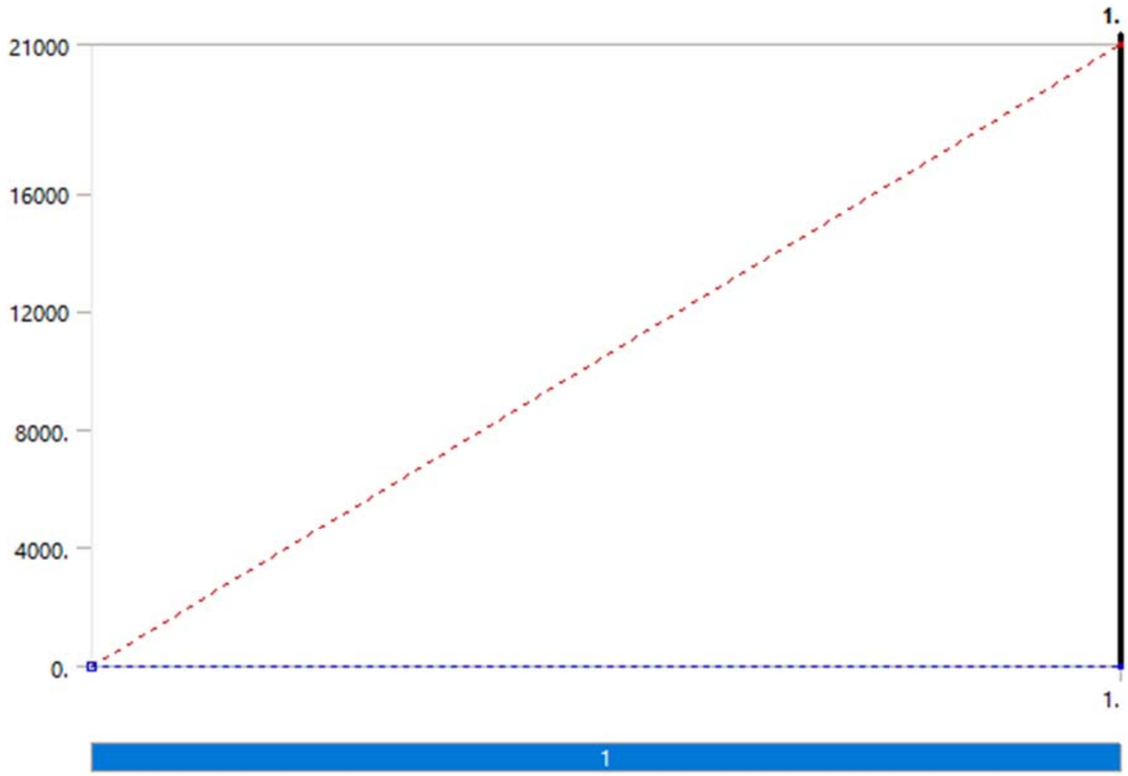

TABLE 13
Model (A4, B4) > Static Structural (A5) > Loads

Object Name	*Cylindrical Support*	*Cylindrical Support 2*
State	Fully Defined	
Scope		
Scoping Method	Named Selection	
Named Selection	bearing1	bearing2
Definition		
Type	Cylindrical Support	
Radial	Fixed	
Axial	Fixed	Free
Tangential	Free	
Suppressed	No	

Solution (A6)

TABLE 14
Model (A4, B4) > Static Structural (A5) > Solution

Object Name	*Solution (A6)*
State	Solved
Adaptive Mesh Refinement	
Max Refinement Loops	1.
Refinement Depth	2.
Information	

Status	Done
MAPDL Elapsed Time	37. s
MAPDL Memory Used	2.834 GB
MAPDL Result File Size	53.375 MB
Post Processing	
Beam Section Results	No
On Demand Stress/Strain	No

TABLE 15
Model (A4, B4) > Static Structural (A5) > Solution (A6) > Solution Information

Object Name	*Solution Information*
State	Solved
Solution Information	
Solution Output	Solver Output
Newton-Raphson Residuals	0
Identify Element Violations	0
Update Interval	2.5 s
Display Points	All
FE Connection Visibility	
Activate Visibility	Yes
Display	All FE Connectors
Draw Connections Attached To	All Nodes
Line Color	Connection Type
Visible on Results	No
Line Thickness	Single
Display Type	Lines

TABLE 16
Model (A4, B4) > Static Structural (A5) > Solution (A6) > Results

Object Name	*Directional Deformation*	*Maximum Principal Stress*
State	Solved	
Scope		
Scoping Method	Geometry Selection	
Geometry	All Bodies	
Definition		
Type	Directional Deformation	Maximum Principal Stress
Orientation	X Axis	
By	Time	
Display Time	Last	
Coordinate System	Coordinate System	
Calculate Time History	Yes	
Identifier		
Suppressed	No	
Results		
Minimum	0. m	0. Pa
Maximum	0. m	0. Pa
Average	0. m	0. Pa
Minimum Occurs On	B2103_rotor_attachment	

Maximum Occurs On	B2103_rotor_attachment	
Information		
Time	1. s	
Load Step	1	
Substep	1	
Iteration Number	1	
Integration Point Results		
Display Option		Averaged
Average Across Bodies		No

FIGURE 2
Model (A4, B4) > Static Structural (A5) > Solution (A6) > Directional Deformation

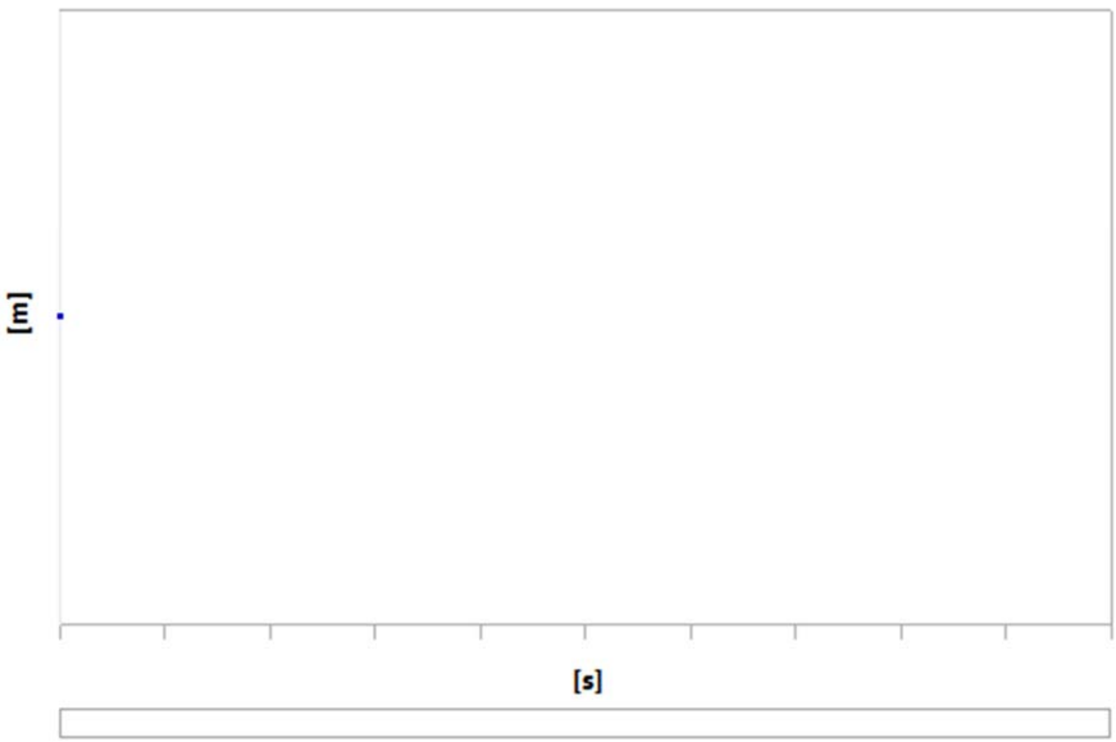

TABLE 17
Model (A4, B4) > Static Structural (A5) > Solution (A6) > Directional Deformation

Time [s]	Minimum [m]	Maximum [m]	Average [m]
1.	0.	0.	0.

FIGURE 3
Model (A4, B4) > Static Structural (A5) > Solution (A6) > Maximum Principal Stress

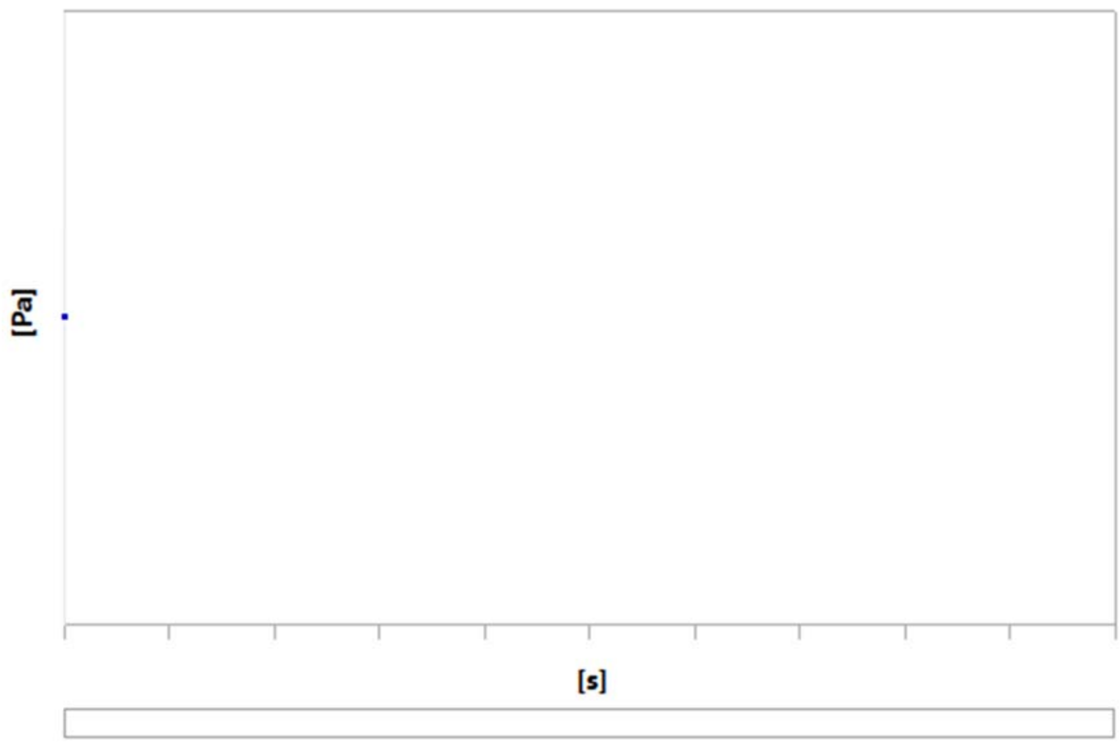

TABLE 18
Model (A4, B4) > Static Structural (A5) > Solution (A6) > Maximum Principal Stress

Time [s]	Minimum [Pa]	Maximum [Pa]	Average [Pa]
1.	0.	0.	0.

Modal (B5)

TABLE 19
Model (A4, B4) > Analysis

Object Name	*Modal (B5)*
State	Solved
Definition	
Physics Type	Structural
Analysis Type	Modal
Solver Target	Mechanical APDL
Options	
Generate Input Only	No

TABLE 20
Model (A4, B4) > Modal (B5) > Initial Condition

Object Name	*Pre-Stress (Static Structural)*
State	Fully Defined
Definition	
Pre-Stress Environment	Static Structural

Pre-Stress Define By	Program Controlled
Reported Loadstep	Last
Reported Substep	Last
Reported Time	End Time
Contact Status	Use True Status
Newton-Raphson Option	Program Controlled

TABLE 21
Model (A4, B4) > Modal (B5) > Analysis Settings

Object Name	*Analysis Settings*
State	Fully Defined
Options	
Max Modes to Find	15
Limit Search to Range	No
Spin Softening	Program Controlled
Solver Controls	
Damped	Yes
Solver Type	Program Controlled
Rotordynamics Controls	
Coriolis Effect	On
Campbell Diagram	On
Number of Points	12
Output Controls	
Stress	No
Strain	No
Nodal Forces	No
Calculate Reactions	No
General Miscellaneous	No
Damping Controls	
Stiffness Coefficient Define By	Direct Input
Stiffness Coefficient	0.
Mass Coefficient	0.
Analysis Data Management	

Solver Files Directory	E:\KeenanHarman\ANSYS\shaft+rotor+balance_piston\shaft+rotor+balance_piston_files\dp0\SYS-1\MECH\
Future Analysis	None
Scratch Solver Files Directory	
Save MAPDL db	No
Contact Summary	Program Controlled
Delete Unneeded Files	Yes
Solver Units	Active System
Solver Unit System	mks

TABLE 22
Model (A4, B4) > Modal (B5) > Rotations

Object Name	*Rotational Velocity*
State	Fully Defined
Scope	
Scoping Method	Geometry Selection
Geometry	All Bodies
Definition	
Define By	Components
Coordinate System	Global Coordinate System
X Component	Tabular Data
Y Component	Tabular Data
Z Component	Tabular Data
X Coordinate	0. m
Y Coordinate	0. m
Z Coordinate	0. m
Suppressed	No

TABLE 23
Model (A4, B4) > Modal (B5) > Rotational Velocity

Points	X [rpm]	Y [rpm]	Z [rpm]
1	0.	0.	0.
2	2000.		
3	4000.		
4	6000.		
5	8000.		
6	10000		
7	12000		
8	14000		
9	16000		

10	18000		
11	20000		
12	21000		

Solution (B6)

TABLE 24
Model (A4, B4) > Modal (B5) > Solution

Object Name	*Solution (B6)*
State	Solved
Adaptive Mesh Refinement	
Max Refinement Loops	1.
Refinement Depth	2.
Information	
Status	Done
MAPDL Elapsed Time	13 m 51 s
MAPDL Memory Used	7.4072 GB
MAPDL Result File Size	1.5539 GB
Post Processing	
Beam Section Results	No

The following bar chart indicates the frequency at each calculated mode.

FIGURE 4
Model (A4, B4) > Modal (B5) > Solution (B6)

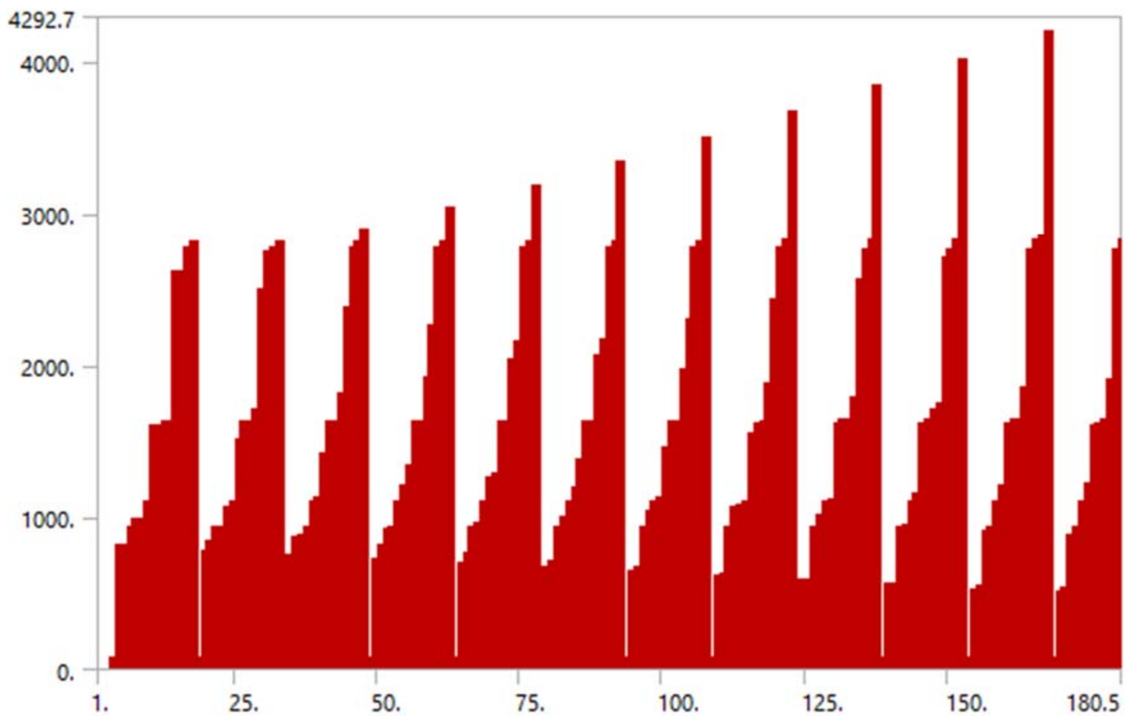

TABLE 25
Model (A4, B4) > Modal (B5) > Solution (B6)

Set	Solve Point	Mode	Damped Frequency [Hz]	Stability [Hz]	Modal Damping Ratio	Logarithmic Decrement
1.	1.	1.	81.335	0.	0.	0.
2.		2.	812.65			
3.		3.	813.92			
4.		4.	937.88			
5.		5.	991.94			
6.		6.	994.15			
7.		7.	1102.3			
8.		8.	1609.1			
9.		9.	1609.4			
10.		10.	1632.2			
11.		11.	1632.7			
12.		12.	2626.1			
13.		13.	2626.9			
14.		14.	2772.7			
15.		15.	2823.7			
16.	2.	1.	81.335			
17.		2.	780.98			
18.		3.	846.93			
19.		4.	929.25			
20.		5.	937.89			
21.		6.	1061.2			
22.		7.	1102.3			
23.		8.	1514.5			
24.		9.	1631.5			
25.		10.	1633.4			
26.		11.	1709.9			
27.		12.	2501.7			
28.		13.	2757.5			
29.		14.	2772.7			
30.		15.	2823.7			
31.	3.	1.	81.335			
32.		2.	750.02			
33.		3.	869.84			
34.		4.	881.89			
35.		5.	937.89			
36.		6.	1102.3			
37.		7.	1133.7			
38.		8.	1425.7			
39.		9.	1630.6			
40.		10.	1634.2			
41.		11.	1816.4			
42.		12.	2383.1			
43.		13.	2772.7			
44.		14.	2823.8			

45.		15.	2894.7			
46.	4.	1.	81.335			
47.		2.	720.38			
48.		3.	814.69			
49.		4.	918.17			
50.		5.	937.89			
51.		6.	1102.3			
52.		7.	1210.4			
53.		8.	1342.7			
54.		9.	1629.7			
55.		10.	1635.1			
56.		11.	1928.7			
57.		12.	2270.7			
58.		13.	2772.6			
59.		14.	2823.9			
60.		15.	3038.			
61.	5.	1.	81.335			
62.		2.	692.05			
63.		3.	763.66			
64.		4.	937.88			
65.		5.	955.78			
66.		6.	1102.3			
67.		7.	1265.3			
68.		8.	1291.3			
69.		9.	1628.8			
70.		10.	1636.			
71.		11.	2046.7			
72.		12.	2164.3			
73.		13.	2772.5			
74.		14.	2824.			
75.		15.	3187.4			
76.	6.	1.	81.335			
77.		2.	664.99			
78.		3.	716.58			
79.		4.	937.88			
80.		5.	994.65			
81.		6.	1102.3			
82.		7.	1193.3			
83.		8.	1376.2			
84.		9.	1627.9			
85.		10.	1636.9			
86.		11.	2063.8			
87.		12.	2170.1			
88.		13.	2772.3			
89.		14.	2824.1			
90.		15.	3342.7			
91.	7.	1.	81.335			

92.		2.	639.2			
93.		3.	673.24			
94.		4.	937.88			
95.		5.	1034.8			
96.		6.	1102.3			
97.		7.	1126.6			
98.		8.	1464.8			
99.		9.	1627.			
100.		10.	1637.9			
101.		11.	1969.			
102.		12.	2298.7			
103.		13.	2772.2			
104.		14.	2824.3			
105.		15.	3503.6			
106.	8.	1.	81.335			
107.		2.	614.63			
108.		3.	633.42			
109.		4.	937.88			
110.		5.	1064.7			
111.		6.	1076.2			
112.		7.	1102.3			
113.		8.	1556.8			
114.		9.	1626.1			
115.		10.	1638.8			
116.		11.	1879.7			
117.		12.	2432.2			
118.		13.	2771.9			
119.		14.	2824.5			
120.		15.	3670.1			
121.	9.	1.	81.335			
122.		2.	591.24			
123.		3.	596.87			
124.		4.	937.88			
125.		5.	1007.5			
126.		6.	1102.3			
127.		7.	1118.7			
128.		8.	1625.2			
129.		9.	1639.7			
130.		10.	1652.2			
131.		11.	1795.6			
132.		12.	2570.4			
133.		13.	2771.7			
134.		14.	2824.8			
135.		15.	3841.8			
136.	10.	1.	81.335			
137.		2.	563.3			
138.		3.	569.04			

139.		4.	937.88			
140.		5.	954.61			
141.		6.	1102.3			
142.		7.	1162.4			
143.		8.	1624.3			
144.		9.	1640.6			
145.		10.	1716.6			
146.		11.	1750.6			
147.		12.	2712.8			
148.		13.	2771.4			
149.		14.	2825.1			
150.		15.	4018.6			
151.	11.	1.	81.335			
152.		2.	532.54			
153.		3.	547.91			
154.		4.	905.71			
155.		5.	937.88			
156.		6.	1102.3			
157.		7.	1207.2			
158.		8.	1623.4			
159.		9.	1641.5			
160.		10.	1642.4			
161.		11.	1851.7			
162.		12.	2771.1			
163.		13.	2825.4			
164.		14.	2859.3			
165.		15.	4200.2			
166.	12.	1.	81.335			
167.		2.	518.12			
168.		3.	537.75			
169.		4.	882.67			
170.		5.	937.88			
171.		6.	1102.3			
172.		7.	1230.			
173.		8.	1607.			
174.		9.	1623.			
175.		10.	1641.9			
176.		11.	1903.3			
177.		12.	2771.			
178.		13.	2825.5			
179.		14.	2933.9			
180.		15.	4292.7			

TABLE 26
Model (A4, B4) > Modal (B5) > Solution (B6) > Solution Information

Object Name	*Solution Information*
State	Solved

Solution Information	
Solution Output	Solver Output
Newton-Raphson Residuals	0
Identify Element Violations	0
Update Interval	2.5 s
Display Points	All
FE Connection Visibility	
Activate Visibility	Yes
Display	All FE Connectors
Draw Connections Attached To	All Nodes
Line Color	Connection Type
Visible on Results	No
Line Thickness	Single
Display Type	Lines

TABLE 27
Model (A4, B4) > Modal (B5) > Solution (B6) > Results

Object Name	*Total Deformation*
State	Solved
Scope	
Scoping Method	Geometry Selection
Geometry	All Bodies
Definition	
Type	Total Deformation
Set Number	1.
Amplitude	No
Sweeping Phase	0. °
Identifier	
Suppressed	No
Results	
Minimum	3.51e-007 m
Maximum	0.69976 m
Average	0.58735 m
Minimum Occurs On	B2105-1_main_drive_shafts
Maximum Occurs On	B2108-3_balance_piston
Information	
Mode	1
Damped Frequency	81.335 Hz
Stability	0. Hz
Modal Damping Ratio	0.
Logarithmic Decrement	0.

TABLE 28
Model (A4, B4) > Modal (B5) > Solution (B6) > Total Deformation

Set	Solve Point	Mode	Damped Frequency [Hz]	Stability [Hz]	Modal Damping Ratio	Logarithmic Decrement
1.	1.	1.	81.335	0.	0.	0.
2.		2.	812.65			

3.		3.	813.92			
4.		4.	937.88			
5.		5.	991.94			
6.		6.	994.15			
7.		7.	1102.3			
8.		8.	1609.1			
9.		9.	1609.4			
10.		10.	1632.2			
11.		11.	1632.7			
12.		12.	2626.1			
13.		13.	2626.9			
14.		14.	2772.7			
15.		15.	2823.7			
16.	2.	1.	81.335			
17.		2.	780.98			
18.		3.	846.93			
19.		4.	929.25			
20.		5.	937.89			
21.		6.	1061.2			
22.		7.	1102.3			
23.		8.	1514.5			
24.		9.	1631.5			
25.		10.	1633.4			
26.		11.	1709.9			
27.		12.	2501.7			
28.		13.	2757.5			
29.		14.	2772.7			
30.		15.	2823.7			
31.	3.	1.	81.335			
32.		2.	750.02			
33.		3.	869.84			
34.		4.	881.89			
35.		5.	937.89			
36.		6.	1102.3			
37.		7.	1133.7			
38.		8.	1425.7			
39.		9.	1630.6			
40.		10.	1634.2			
41.		11.	1816.4			
42.		12.	2383.1			
43.		13.	2772.7			
44.		14.	2823.8			
45.		15.	2894.7			
46.	4.	1.	81.335			
47.		2.	720.38			
48.		3.	814.69			
49.		4.	918.17			

50.		5.	937.89			
51.		6.	1102.3			
52.		7.	1210.4			
53.		8.	1342.7			
54.		9.	1629.7			
55.		10.	1635.1			
56.		11.	1928.7			
57.		12.	2270.7			
58.		13.	2772.6			
59.		14.	2823.9			
60.		15.	3038.			
61.	5.	1.	81.335			
62.		2.	692.05			
63.		3.	763.66			
64.		4.	937.88			
65.		5.	955.78			
66.		6.	1102.3			
67.		7.	1265.3			
68.		8.	1291.3			
69.		9.	1628.8			
70.		10.	1636.			
71.		11.	2046.7			
72.		12.	2164.3			
73.		13.	2772.5			
74.		14.	2824.			
75.		15.	3187.4			
76.	6.	1.	81.335			
77.		2.	664.99			
78.		3.	716.58			
79.		4.	937.88			
80.		5.	994.65			
81.		6.	1102.3			
82.		7.	1193.3			
83.		8.	1376.2			
84.		9.	1627.9			
85.		10.	1636.9			
86.		11.	2063.8			
87.		12.	2170.1			
88.		13.	2772.3			
89.		14.	2824.1			
90.		15.	3342.7			
91.	7.	1.	81.335			
92.		2.	639.2			
93.		3.	673.24			
94.		4.	937.88			
95.		5.	1034.8			
96.		6.	1102.3			

97.		7.	1126.6			
98.		8.	1464.8			
99.		9.	1627.			
100.		10.	1637.9			
101.		11.	1969.			
102.		12.	2298.7			
103.		13.	2772.2			
104.		14.	2824.3			
105.		15.	3503.6			
106.	8.	1.	81.335			
107.		2.	614.63			
108.		3.	633.42			
109.		4.	937.88			
110.		5.	1064.7			
111.		6.	1076.2			
112.		7.	1102.3			
113.		8.	1556.8			
114.		9.	1626.1			
115.		10.	1638.8			
116.		11.	1879.7			
117.		12.	2432.2			
118.		13.	2771.9			
119.		14.	2824.5			
120.		15.	3670.1			
121.	9.	1.	81.335			
122.		2.	591.24			
123.		3.	596.87			
124.		4.	937.88			
125.		5.	1007.5			
126.		6.	1102.3			
127.		7.	1118.7			
128.		8.	1625.2			
129.		9.	1639.7			
130.		10.	1652.2			
131.		11.	1795.6			
132.		12.	2570.4			
133.		13.	2771.7			
134.		14.	2824.8			
135.		15.	3841.8			
136.	10.	1.	81.335			
137.		2.	563.3			
138.		3.	569.04			
139.		4.	937.88			
140.		5.	954.61			
141.		6.	1102.3			
142.		7.	1162.4			
143.		8.	1624.3			

144.		9.	1640.6			
145.		10.	1716.6			
146.		11.	1750.6			
147.		12.	2712.8			
148.		13.	2771.4			
149.		14.	2825.1			
150.		15.	4018.6			
151.	11.	1.	81.335			
152.		2.	532.54			
153.		3.	547.91			
154.		4.	905.71			
155.		5.	937.88			
156.		6.	1102.3			
157.		7.	1207.2			
158.		8.	1623.4			
159.		9.	1641.5			
160.		10.	1642.4			
161.		11.	1851.7			
162.		12.	2771.1			
163.		13.	2825.4			
164.		14.	2859.3			
165.		15.	4200.2			
166.	12.	1.	81.335			
167.		2.	518.12			
168.		3.	537.75			
169.		4.	882.67			
170.		5.	937.88			
171.		6.	1102.3			
172.		7.	1230.			
173.		8.	1607.			
174.		9.	1623.			
175.		10.	1641.9			
176.		11.	1903.3			
177.		12.	2771.			
178.		13.	2825.5			
179.		14.	2933.9			
180.		15.	4292.7			

TABLE 29
Model (A4, B4) > Modal (B5) > Solution (B6) > Result Charts

Object Name	*Campbell Diagram*
State	Solved
Scope	
Rotational Velocity Selection	Rotational Velocity
Campbell Diagram Controls	
Y Axis Data	Frequency
Critical Speed	Yes

Ratio	2.
Sorting	Yes
Axis	
X Axis Label	Rotational Velocity
X Axis Range	Program Controlled
X Axis Minimum	0. RPM
X Axis Maximum	21000 RPM
Y Axis Label	Frequency
Y Axis Range	Program Controlled
Y Axis Minimum	0. Hz
Y Axis Maximum	4292.7 Hz
Definition	
Suppressed	No

FIGURE 5
Model (A4, B4) > Modal (B5) > Solution (B6) > Campbell Diagram

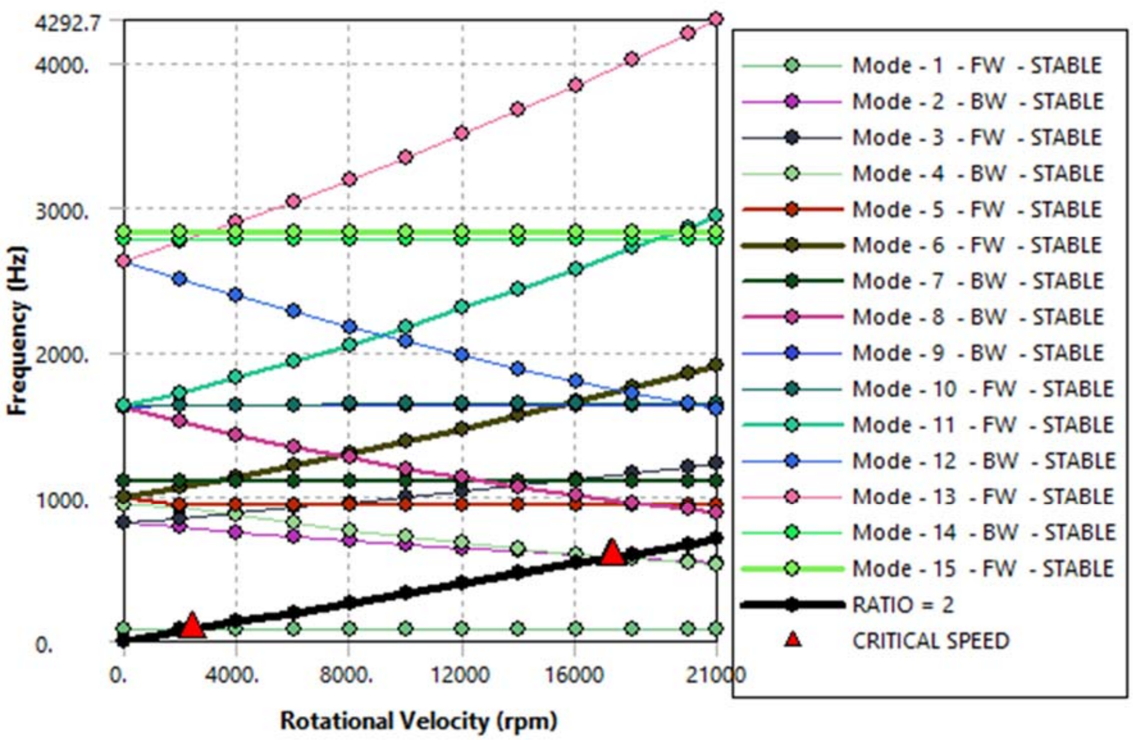

Model (A4, B4) > Modal (B5) > Solution (B6) > Campbell Diagram

Mode	Whirl Direction	Mode Stability	Critical Speed	0. rpm	2000. rpm	4000. rpm	6000. rpm	8000. rpm	10000 rpm	12000 rpm	14000 rpm	16000 rpm	18000 rpm	20000 rpm	21000 rpm
1.	FW	STABLE	2440.1 rpm	81.335 Hz	81.335 Hz	81.335 Hz	81.335 Hz	81.335 Hz	81.335 Hz	81.335 Hz	81.335 Hz	81.335 Hz	81.335 Hz	81.335 Hz	81.335 Hz

2.	BW	STABLE	17303 rpm	812.65 Hz	780.98 Hz	750.02 Hz	720.38 Hz	692.05 Hz	664.99 Hz	639.2 Hz	614.63 Hz	591.24 Hz	569.04 Hz	547.91 Hz	537.75 Hz
3.	FW	STABLE	NONE	813.92 Hz	846.93 Hz	881.89 Hz	918.17 Hz	955.78 Hz	994.65 Hz	1034.8 Hz	1076.2 Hz	1118.7 Hz	1162.4 Hz	1207.2 Hz	1230. Hz
4.	BW	STABLE	17268 rpm	937.88 Hz	929.25 Hz	869.84 Hz	814.69 Hz	763.66 Hz	716.58 Hz	673.24 Hz	633.42 Hz	596.87 Hz	563.3 Hz	532.54 Hz	518.12 Hz
5.	FW	STABLE	NONE	991.94 Hz	937.89 Hz	937.89 Hz	937.89 Hz	937.88 Hz	937.88 Hz	937.88 Hz	937.88 Hz	937.88 Hz	937.88 Hz	937.88 Hz	937.88 Hz
6.	FW	STABLE	NONE	994.15 Hz	1061.2 Hz	1133.7 Hz	1210.4 Hz	1291.3 Hz	1376.2 Hz	1464.8 Hz	1556.8 Hz	1652.2 Hz	1750.6 Hz	1851.7 Hz	1903.3 Hz
7.	BW	STABLE	NONE	1102.3 Hz	1102.3 Hz	1102.3 Hz	1102.3 Hz	1102.3 Hz	1102.3 Hz	1102.3 Hz	1102.3 Hz	1102.3 Hz	1102.3 Hz	1102.3 Hz	1102.3 Hz
8.	BW	STABLE	NONE	1609.1 Hz	1514.5 Hz	1425.7 Hz	1342.7 Hz	1265.3 Hz	1193.3 Hz	1126.6 Hz	1064.7 Hz	1007.5 Hz	954.61 Hz	905.71 Hz	882.67 Hz
9.	BW	STABLE	NONE	1609.4 Hz	1631.5 Hz	1630.6 Hz	1629.7 Hz	1628.8 Hz	1627.9 Hz	1627. Hz	1626.1 Hz	1625.2 Hz	1624.3 Hz	1623.4 Hz	1623. Hz
10.	FW	STABLE	NONE	1632.2 Hz	1633.4 Hz	1634.2 Hz	1635.1 Hz	1636. Hz	1636.9 Hz	1637.9 Hz	1638.8 Hz	1639.7 Hz	1640.6 Hz	1641.5 Hz	1641.9 Hz
11.	FW	STABLE	NONE	1632.7 Hz	1709.9 Hz	1816.4 Hz	1928.7 Hz	2046.7 Hz	2170.1 Hz	2298.7 Hz	2432.2 Hz	2570.4 Hz	2712.8 Hz	2859.3 Hz	2933.9 Hz
12.	BW	STABLE	NONE	2626.1 Hz	2501.7 Hz	2383.1 Hz	2270.7 Hz	2164.3 Hz	2063.8 Hz	1969. Hz	1879.7 Hz	1795.6 Hz	1716.6 Hz	1642.4 Hz	1607. Hz
13.	FW	STABLE	NONE	2626.9 Hz	2757.5 Hz	2894.7 Hz	3038. Hz	3187.4 Hz	3342.7 Hz	3503.6 Hz	3670.1 Hz	3841.8 Hz	4018.6 Hz	4200.2 Hz	4292.7 Hz
14.	BW	STABLE	NONE	2772.7 Hz	2772.7 Hz	2772.7 Hz	2772.6 Hz	2772.5 Hz	2772.3 Hz	2772.2 Hz	2771.9 Hz	2771.7 Hz	2771.4 Hz	2771.1 Hz	2771. Hz
15.	FW	STABLE	NONE	2823.7 Hz	2823.7 Hz	2823.8 Hz	2823.9 Hz	2824. Hz	2824.1 Hz	2824.3 Hz	2824.5 Hz	2824.8 Hz	2825.1 Hz	2825.4 Hz	2825.5 Hz

Material Data

Structural Steel

TABLE 30
Structural Steel > Constants

Density	7850 kg m^-3

Isotropic Secant Coefficient of Thermal Expansion	1.2e-005 C^-1
Specific Heat Constant Pressure	434 J kg^-1 C^-1
Isotropic Thermal Conductivity	60.5 W m^-1 C^-1
Isotropic Resistivity	1.7e-007 ohm m

TABLE 31
Structural Steel > Color

Red	Green	Blue
132	139	179

TABLE 32
Structural Steel > Compressive Ultimate Strength

Compressive Ultimate Strength Pa
0

TABLE 33
Structural Steel > Compressive Yield Strength

Compressive Yield Strength Pa
2.5e+008

TABLE 34
Structural Steel > Tensile Yield Strength

Tensile Yield Strength Pa
2.5e+008

TABLE 35
Structural Steel > Tensile Ultimate Strength

Tensile Ultimate Strength Pa
4.6e+008

TABLE 36
Structural Steel > Isotropic Secant Coefficient of Thermal Expansion

Zero-Thermal-Strain Reference Temperature C
22

TABLE 37
Structural Steel > S-N Curve

Alternating Stress Pa	Cycles	Mean Stress Pa
3.999e+009	10	0
2.827e+009	20	0
1.896e+009	50	0
1.413e+009	100	0
1.069e+009	200	0
4.41e+008	2000	0
2.62e+008	10000	0
2.14e+008	20000	0
1.38e+008	1.e+005	0
1.14e+008	2.e+005	0

8.62e+007	1.e+006	0

TABLE 38
Structural Steel > Strain-Life Parameters

Strength Coefficient Pa	Strength Exponent	Ductility Coefficient	Ductility Exponent	Cyclic Strength Coefficient Pa	Cyclic Strain Hardening Exponent
9.2e+008	-0.106	0.213	-0.47	1.e+009	0.2

TABLE 39
Structural Steel > Isotropic Elasticity

Young's Modulus Pa	Poisson's Ratio	Bulk Modulus Pa	Shear Modulus Pa	Temperature C
2.e+011	0.3	1.6667e+011	7.6923e+010	

TABLE 40
Structural Steel > Isotropic Relative Permeability

Relative Permeability
10000

THIS PAGE INTENTIONALLY LEFT BLANK

APPENDIX B. ANSYS REPORT DATA FOR CFX ANALYSIS

1. File Report

Table 1. File Information for CFX

Case	CFX
File Path	E:\KeenanHarman\New_test_ring\ME4225\balance_piston_flow_slice_4_1bar_run2_files\dp0\CFX\CFX\Fluid Flow CFX_008.res
File Date	03 June 2019
File Time	12:23:52 PM
File Type	CFX5
File Version	19.2

2. Mesh Report

Table 2. Mesh Information for CFX

Domain	Nodes	Elements
Default Domain	266959	1362329

3. Physics Report

Table 3. Domain Physics for CFX

Domain - Default Domain	
Type	Fluid
Location	B219
Materials	
Air Ideal Gas	
Fluid Definition	Material Library
Morphology	Continuous Fluid
Settings	
Buoyancy Model	Non Buoyant
Domain Motion	Rotating
Angular Velocity	2.1000e+04 [rev min^-1]
Axis Definition	Coordinate Axis
Rotation Axis	Coord 0.1
Reference Pressure	1.0000e+00 [atm]
Heat Transfer Model	Total Energy
Include Viscous Work Term	True
Turbulence Model	k epsilon
Turbulent Wall Functions	Scalable
High Speed Model	Off
Domain Interface - Periodic	
Boundary List1	Periodic Side 1
Boundary List2	Periodic Side 2
Interface Type	Fluid Fluid
Settings	
Interface Models	Rotational Periodicity
Axis Definition	Coordinate Axis
Rotation Axis	Coord 0.1
Mesh Connection	Automatic

Table 4. Boundary Physics for CFX

Domain	**Boundaries**
	Boundary - Inlet

Default Domain	Type	INLET
	Location	Inlet
	Settings	
	Flow Direction	Normal to Boundary Condition
	Flow Regime	Subsonic
	Heat Transfer	Stationary Frame Total Temperature
	Stationary Frame Total Temperature	2.8815e+02 [K]
	Mass And Momentum	Stationary Frame Total Pressure
	Relative Pressure	3.0000e+00 [bar]
	Turbulence	Medium Intensity and Eddy Viscosity Ratio
	Boundary - Periodic Side 1	
	Type	INTERFACE
	Location	Sym1
	Settings	
	Heat Transfer	Conservative Interface Flux
	Mass And Momentum	Conservative Interface Flux
	Turbulence	Conservative Interface Flux
	Boundary - Periodic Side 2	
	Type	INTERFACE
	Location	Sym2
	Settings	
	Heat Transfer	Conservative Interface Flux
	Mass And Momentum	Conservative Interface Flux
	Turbulence	Conservative Interface Flux
	Boundary - Outlet	
	Type	OPENING
	Location	Outlet
	Settings	
	Flow Direction	Normal to Boundary Condition
	Flow Regime	Subsonic

	Heat Transfer	Opening Temperature
	Opening Temperature	2.8815e+02 [K]
	Mass And Momentum	Opening Pressure and Direction
	Relative Pressure	0.0000e+00 [bar]
	Turbulence	Medium Intensity and Eddy Viscosity Ratio
	Boundary - Default Domain Default	
	Type	WALL
	Location	F161.219, F162.219, F163.219, F169.219, F170.219, F172.219, F173.219, F174.219, F175.219, F176.219, F177.219, F178.219, F179.219, F180.219, F181.219, F182.219, F183.219, F184.219, F185.219, F186.219, F187.219, F188.219, F189.219, F190.219, F191.219, F192.219, F193.219, F195.219, F196.219, F197.219, F198.219, F199.219, F200.219, F201.219, F202.219, F203.219, F204.219, F205.219, F207.219, F208.219, F209.219, F210.219, F211.219, F212.219, F213.219, F214.219
	Settings	
	Heat Transfer	Adiabatic
	Mass And Momentum	No Slip Wall
	Wall Roughness	Smooth Wall
	Boundary - Stationary	
	Type	WALL
	Location	Stationary
	Settings	
	Heat Transfer	Adiabatic
	Mass And Momentum	No Slip Wall
	Wall Velocity	Counter Rotating Wall
	Wall Roughness	Smooth Wall

LIST OF REFERENCES

[1] A. Byrd. "Modernization of the Transonic Axial Compressor Test Rig." Master's Thesis, Department of Mechanical and Aerospace Engineering, Naval Postgraduate School, Monterey, CA, 2017. http://hdl.handle.net/10945/56876

[2] A. J. Gannon and G. V. Hobson, "Performance Testing of Transonic Rotors," *Mech. Eng.,* pp. 52–53, 2010. Available: http://libproxy.nps.edu/login?url= https://search.proquest.com/docview/742466821?accountid=12702.

[3] J. Cameron et al. "A Transonic Axial Compressor Facility for Fundamental Research and Flow Control Development." *44th AIAA Aerospace Sciences Meeting and Exhibit,* 2006. Available: https://doi.org/10.2514/6.2006-416

[4] "Transonic Compressor 1," Technische Universität Darmstadt. Accessed June 6th, 2019. [Online]. Available: https://www.glr.tu-darmstadt.de/glr_forschung/verdichter/tsv1/index.en.jsp

[5] R. A. Brokopp. "NASA Glenn's Single-Stage Axial Compressor Facility Upgraded." *Research and Technology,* 2003. Available: http://hdl.handle.net/2060/20050215485.

[6] "Compressor Research Facility (CRF)," Aerospace Systems Directorate. Accessed June 6th, 2019. [Online]. Available: https://www.wpafb.af.mil/Portals/60/documents/afrl/rq/wpafb/rq-compressor-research-CRF-%202018.pdf?ver=2018-07-06-132112-140

[7] B. Grossman. "Testing and Analysis of a Transonic Axial Compressor." Master's Thesis, Department of Aeronautical Engineering, Naval Postgraduate School, Monterey, CA, 1997. http://hdl.handle.net/10945/9064

THIS PAGE INTENTIONALLY LEFT BLANK

INITIAL DISTRIBUTION LIST

1. Defense Technical Information Center
   Ft. Belvoir, Virginia

2. Dudley Knox Library
   Naval Postgraduate School
   Monterey, California